Global Biogeochemical Cycles®

RESEARCH ARTICLE
10.1029/2021GB007113

Carbon Accumulation, Flux, and Fate in Stordalen Mire, a Permafrost Peatland in Transition

M. E. Holmes[1,2], P. M. Crill[3], W. C. Burnett[1], C. K. McCalley[4], R. M. Wilson[1], S. Frolking[5], K.-Y. Chang[6], W. J. Riley[6], R. K. Varner[5], S. B. Hodgkins[7], IsoGenie Project Coordinators[8], IsoGenie Field Team[9], A. P. McNichol[10], S. R. Saleska[11], V. I. Rich[7,12], and J. P. Chanton[1]

[1]Department of Earth, Ocean, and Atmospheric Science, Florida State University, Tallahassee, FL, USA, [2]Now at Science and Math Division, Tallahassee Community College, Tallahassee, FL, USA, [3]Department of Geological Sciences and Bolin Centre for Climate Research, Stockholm University, Stockholm, Sweden, [4]Thomas H. Gosnell School of Life Sciences, Rochester Institute of Technology, Rochester, NY, USA, [5]Earth Systems Research Center, Institute for the Study of Earth, Oceans and Space, and Department of Earth Sciences, University of New Hampshire, Durham, NH, USA, [6]Climate and Ecosystem Sciences Division, Lawrence Berkeley National Laboratory, Berkeley, CA, USA, [7]Department of Microbiology, The Ohio State University, Columbus, OH, USA, [8]See Appendix A, [9]See Appendix B, [10]Woods Hole Oceanographic Institution, Woods Hole, MA, USA, [11]Department of Ecology and Evolutionary Biology, University of Arizona, Tucson, AZ, USA, [12]Department of Soil, Water and Environmental Sciences, University of Arizona, Tucson, AZ, USA

Key Points:

- Stordalen Mire, a permafrost peatland, has become a stronger carbon sink due to shifts in vegetation and inundation accompanying thaw
- This stronger carbon sink is offset by an increase in methane emission, resulting in higher net $CO_{2\text{-equivalent}}$ emissions
- Analysis of respiration products indicates that methane emission from the fen and bog are dominated by modern carbon

Supporting Information:

Supporting Information may be found in the online version of this article.

Correspondence to:

M. E. Holmes,
beth.huettel@tcc.fl.edu

Citation:

Holmes, M. E., Crill, P. M., Burnett, W. C., McCalley, C. K., Wilson, R. M., Frolking, S., et al. (2022). Carbon accumulation, flux, and fate in Stordalen Mire, a permafrost peatland in transition. *Global Biogeochemical Cycles*, *36*, e2021GB007113. https://doi.org/10.1029/2021GB007113

Received 30 JUN 2021
Accepted 20 DEC 2021

Author Contributions:

Conceptualization: M. E. Holmes, P. M. Crill, S. Frolking, K.-Y. Chang, W. J. Riley, R. K. Varner, S. R. Saleska, V. I. Rich, J. P. Chanton
Data curation: P. M. Crill, S. B. Hodgkins, V. I. Rich
Formal analysis: M. E. Holmes, P. M. Crill, W. C. Burnett, R. M. Wilson, S. Frolking, K.-Y. Chang, R. K. Varner, V. I. Rich, J. P. Chanton
Funding acquisition: P. M. Crill, S. Frolking, W. J. Riley, R. K. Varner, S. R. Saleska, V. I. Rich, J. P. Chanton
Investigation: M. E. Holmes, P. M. Crill, W. C. Burnett, C. K. McCalley, S. Frolking, K.-Y. Chang, R. K. Varner, S. B. Hodgkins, V. I. Rich, J. P. Chanton

Abstract Stordalen Mire is a peatland in the discontinuous permafrost zone in arctic Sweden that exhibits a habitat gradient from permafrost palsa, to *Sphagnum* bog underlain by permafrost, to *Eriophorum*-dominated fully thawed fen. We used three independent approaches to evaluate the annual, multi-decadal, and millennial apparent carbon accumulation rates (aCAR) across this gradient: seven years of direct semi-continuous measurement of CO_2 and CH_4 exchange, and 21 core profiles for ^{210}Pb and ^{14}C peat dating. Year-round chamber measurements indicated net carbon balance of -13 ± 8, -49 ± 15, and -91 ± 43 g C m^{-2} y^{-1} for the years 2012–2018 in palsa, bog, and fen, respectively. Methane emission offset 2%, 7%, and 17% of the CO_2 uptake rate across this gradient. Recent aCAR indicates higher C accumulation rates in surface peats in the palsa and bog compared to current CO_2 fluxes, but these assessments are more similar in the fen. aCAR increased from low millennial-scale levels (17–29 g C m^{-2} y^{-1}) to moderate aCAR of the past century (72–81 g C m^{-2} y^{-1}) to higher recent aCAR of 90–147 g C m^{-2} y^{-1}. Recent permafrost collapse, greater inundation and vegetation response has made the landscape a stronger CO_2 sink, but this CO_2 sink is increasingly offset by rising CH_4 emissions, dominated by modern carbon as determined by ^{14}C. The higher CH_4 emissions result in higher net $CO_{2\text{-equivalent}}$ emissions, indicating that radiative forcing of this mire and similar permafrost ecosystems will exert a warming influence on future climate.

1. Introduction

The northern circumpolar permafrost zone has been a large long-term sink for carbon (C) and contains ~1,700 Pg of C within the upper 3 m depth, more than twice the amount that is in today's atmosphere (Hugelius et al., 2014; Mishra et al., 2017; Schuur et al., 2013). Permafrost, with its large quantities of stored C (Tarnocai et al., 2009; Zimov et al., 2006), is susceptible to thawing with climate warming (Turetsky et al., 2020). Northern permafrost soils are predicted to release billions of tons of C by 2100, an amount that would significantly increase the atmospheric carbon dioxide (CO_2) burden and affect global climate (McGuire et al., 2018; Schaefer et al., 2014; Schuur et al., 2013) if it is not offset by concurrent plant C assimilation (Grant et al., 2019; Mekonnen et al., 2018) and sequestration in peat and sediments.

Some permafrost soils are composed of peat, where C is particularly concentrated. High latitude peatlands have been accumulating C for thousands of years since deglaciation and have been important in the global carbon cycle throughout the Holocene (MacDonald et al., 2006; Yu, 2011). Expanding knowledge of how these peatlands have reacted in the past with respect to C sequestration and release under changing climatic conditions is important for understanding any feedback effect they may exert in the future.

The C budget in frozen or thawed peatlands depends on the balance between fixation and accumulation of atmospheric C by photosynthesis and loss via respiration and transport, including diffusive, advective, ebullitive, and

Methodology: M. E. Holmes, P. M. Crill, W. C. Burnett, C. K. McCalley, R. M. Wilson, S. Frolking, K.-Y. Chang, W. J. Riley, R. K. Varner, S. B. Hodgkins, A. P. McNichol, J. P. Chanton
Project Administration: P. M. Crill, W. J. Riley, R. K. Varner, S. R. Saleska, V. I. Rich, J. P. Chanton
Resources: P. M. Crill, S. B. Hodgkins, V. I. Rich, J. P. Chanton
Software: K.-Y. Chang, W. J. Riley
Supervision: P. M. Crill, W. C. Burnett, W. J. Riley, V. I. Rich, J. P. Chanton
Validation: P. M. Crill, W. C. Burnett, S. Frolking, J. P. Chanton
Visualization: P. M. Crill, S. Frolking, J. P. Chanton
Writing – original draft: M. E. Holmes, W. C. Burnett, K.-Y. Chang, R. K. Varner, J. P. Chanton
Writing – review & editing: M. E. Holmes, P. M. Crill, W. C. Burnett, C. K. McCalley, R. M. Wilson, S. Frolking, K.-Y. Chang, W. J. Riley, R. K. Varner, S. R. Saleska, V. I. Rich, J. P. Chanton

plant transport mechanisms. Carbon can be lost by decomposition and efflux to the atmosphere in the form of CO_2 or methane (CH_4), or through export of dissolved organic carbon (DOC) or dissolved inorganic carbon (DIC) (Freeman et al., 2001, 2004; Hodgkins et al., 2016; Roulet et al., 2007). During the Holocene, primary production and C sequestration into plant litter and histosols outweighed C losses in high-latitude peat, in large part because of low decomposition rates due to cold temperatures, high soil moisture, and low O_2 availability. Organic matter is also preserved in high latitude wetlands partly due to the acidic metabolites produced by *Sphagnum* spp., a common species (Fudyma et al., 2019). These metabolites inhibit decomposition (Hodgkins et al., 2016; Verhoeven & Liefveld, 1997). Increasing air and soil temperatures are now causing permafrost peatlands to thaw and active layers to thicken, with wide-ranging effects on hydrology, vegetation, decomposition, and gas fluxes (Åkerman & Johansson, 2008; Malhotra et al., 2018; Malmer et al., 2005; Silvola et al., 1996). The warmer temperatures that have been recorded over the past few decades may change some of these areas into C sources as the previously frozen C thaws and decomposes (Dorrepaal et al., 2009).

Carbon released from peatlands is expected to be mainly in the form of CO_2, but a substantial portion is emitted as CH_4 with warming when permafrost thaw leads to subsidence of peat surfaces and waterlogged soils (Olefeldt et al., 2013; Turetsky et al., 2020; von Deimling et al., 2015; Wilson et al., 2016; Wilson, Tfaily, et al., 2021). Methane has a roughly 27 times higher global warming potential on a 100-year period than CO_2 (Forster et al., 2021), so even the small amounts of CH_4 projected to be released from peatlands can significantly impact climate forcing over decadal timescales. Predictions of the effect of C released as CH_4 from thawing permafrost vary. Schaefer et al. (2014) estimated that this CH_4 will contribute no more than 16% of the warming caused by thawing permafrost, while compilations by Schuur et al. (2013) are between 30% and 50%. In addition, permafrost thaw, collapse, and water inundation can result in the formation of ponds and wetlands, with subsequent higher net ecosystem productivity, possible C storage and coincidently elevated CH_4 emission rates (Bäckstrand et al., 2010; Burke et al., 2019; Whiting & Chanton, 1993; Wilson et al., 2017).

Stordalen Mire is an extensively studied, dynamic ecosystem in the discontinuous permafrost zone of sub-arctic Sweden, with environmental records dating back more than a century. The ecosystem community structures of the mire are particularly sensitive to changing climate due to its location on the southern edge of the circumpolar permafrost zone. The sub-ecosystems (which we will call habitats) in the mire range from raised palsas to ombrotrophic bogs with an underlying core of permafrost and permafrost-free minerotrophic fens. Unlike palsas and ombrotrophic bogs, minerotrophic fens receive water not only from precipitation, but also from groundwater and streams. The C fluxes in each of these habitats are distinct because differences in abiotic conditions result in vegetation and microbial community differences (Malhotra & Roulet, 2015; McCalley et al., 2014). Investigations of Stordalen Mire's C balance have differed in their conclusions: some determined it to be a source of C to the atmosphere (Bäckstrand et al., 2010; Malmer & Wallén, 1996), others that it is a sink (Christensen et al., 2012; Olefeldt et al., 2012; Varner et al., 2021).

The objective of this study was to compare three different measures of C accumulation rates in different habitats across a peatland permafrost thaw gradient that spans permafrost palsa, to *Sphagnum*-dominated bog underlain by permafrost, to fully thawed *Eriophorum*-dominated fen in Stordalen Mire. We use ^{210}Pb and ^{14}C to compare C accumulation rates across the three peatland environments over the past several decades to the accumulation over the past hundred to thousands of years. Methane and CO_2 chamber flux measurements give information on current gas fluxes on an annual basis and, together with the radiotracer information, provide insights into the C budget of the mire, which is important for understanding the response of these northern peatlands to changing climatic conditions. We hypothesized that across the thaw, moisture and vegetation gradient (palsa, bog, fen), C deposition and uptake would increase while being offset by methane emissions, particularly affecting the global warming potential of the wetland complex.

2. Materials and Methods

2.1. Study Site

Stordalen Mire in northern Sweden is located at 68°20'N, 19°03'E (Figure 1). Inception of peat deposition in Stordalen Mire occurred between 6,000 and 4,700 years BP (Kokfelt et al., 2010). The Little Ice Age affected this region beginning about 850 years BP, and permafrost formation occurred after 700 years BP (Kokfelt et al., 2010). Prior to permafrost formation, the area may have been dominated by fen vegetation, which

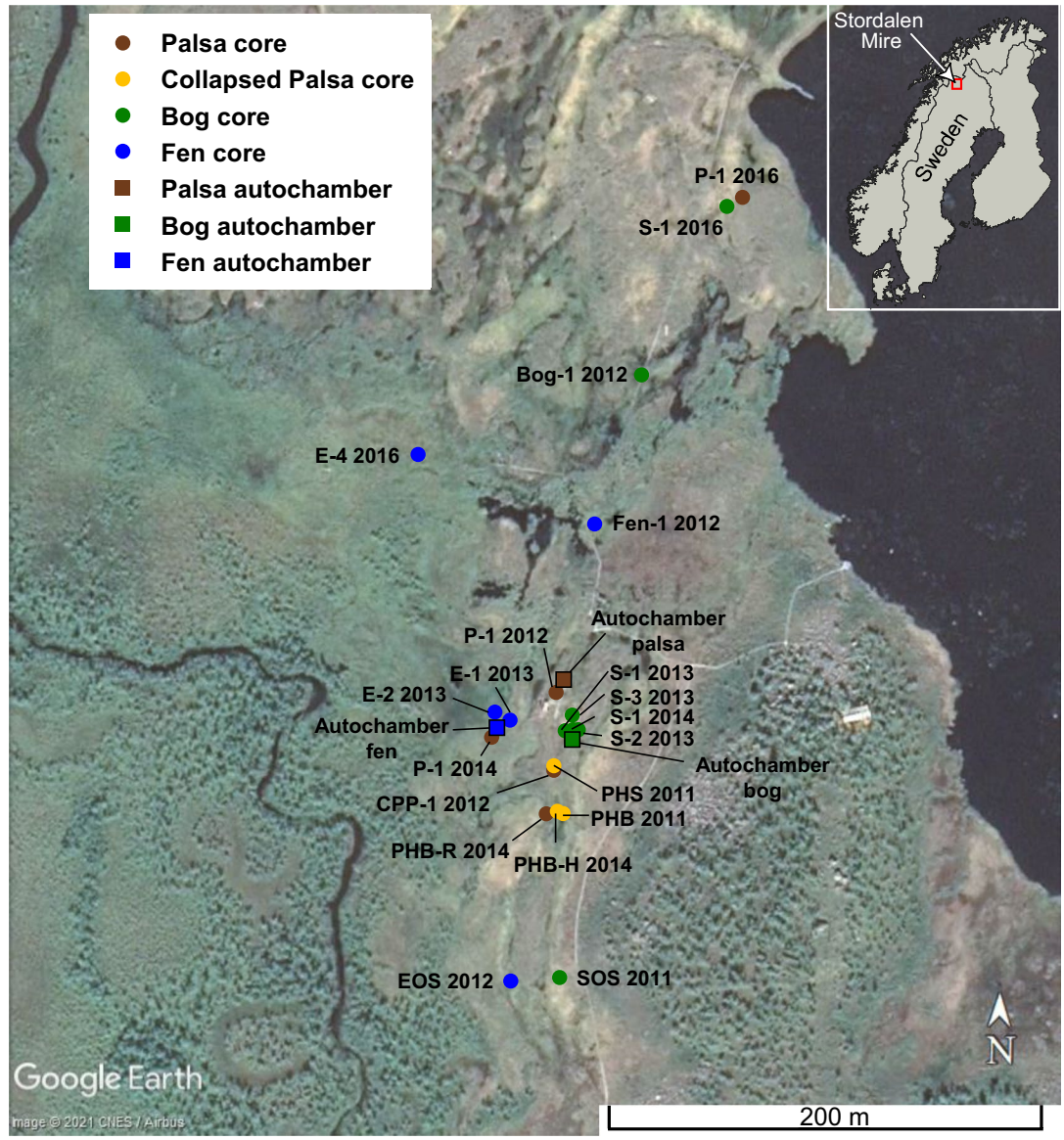

Figure 1. Image of Stordalen Mire showing sample locations of cores on which ^{210}Pb and ^{14}C chronology was determined. Following the approach of Hodgkins et al. (2014), we sampled a range of sites across the mire to capture variability within each of the habitats (i.e., palsa, collapsed palsa, bog, fen), without oversampling and destroying the area around the autochambers. Each sampling location is labeled with its type (P-1, PHB-R, CPP-1 = palsa; PHB-H, PHS, PHB = collapsed palsa; S-1, S-2, S-3, Bog-1, SOS = bog; E-1, E-2, E-3, E-4, EOS, Fen-1 = fen) and year of sampling.

transitioned to palsa with permafrost development and the formation of ombrotrophic peat (Kokfelt et al., 2010; Malmer and Wallén, 1996; Sim et al., 2021). With current increases in temperature in the region (Christensen et al., 2004), changes in mire topography, active layer thickness, hydrology, and vegetation have been well documented since the 1970's (Christensen et al., 2004; Johansson et al., 2006; Malmer et al., 2005; Varner et al., 2021).

Currently, peat in Stordalen Mire is 1–3 m thick (Johansson et al., 2006). About half of the mire currently consists of palsa with an ice-rich permafrost core, with typical seasonal thaw depths of ~50–80 cm. Ericaceous shrubs and cryptogams (mosses and lichens) dominate palsa vegetation. As the permafrost that supports the central palsa of the mire thaws, the surface structure subsides and the palsa collapses and becomes wetter (collapsed palsa; Hodgkins et al., 2014). Bog sites overlie permafrost, which separates them from the water table of the surrounding peatland complex, and are ombrotrophic with nutrients only available from rain, snow, and dustfall deposition. Vegetation in the bog sites is dominated by *Sphagnum* spp., feather mosses (e.g., *Dicranum elongatum*), and

sedges (e.g., *Eriophorum vaginatum* and *Carex biglowii*). At our bog site we find ice consistently in mid-summer at 150 cm, and often at more shallow depths, from 75-100 cm as measured with a steel rod. The bog likely formed from thaw of the palsa habitat, collapse and then refreezing at depth due to the insulating properties of the *Sphagnum* moss. Fully thawed, minerotrophic fens are connected to the water table and are thus more nutrient-rich. Porewater in the fen sites has higher pH than in the bogs. Fen sites are also more productive and are inhabited by sedges such as *Eriophorum angustifolium, Carex rostrata*, and *Esquisetum* spp., as well as *Sphagnum* spp. (Johansson et al., 2006; Malhotra & Roulet, 2015; Malmer et al., 2005). In this study, we conducted flux measurements in palsa, bog, and fen and we cored palsa, collapsed palsa, bog, and fen sites. Overall, we divide the mire into three main habitats: palsa (including collapsed palsa), bog, and fen.

2.2. Core and Porewater Sampling

Twenty-one peat cores were collected from Stordalen Mire for measurements of ^{210}Pb and ^{14}C (Table S1 in Supporting Information S1). In three of the cores (collected in 2016 from a palsa, a bog, and a fen), both ^{210}Pb and ^{14}C were measured in 1 cm sections in the upper 10 cm, and 2 cm sections below 10 cm. The 2016 cores were cut from the surrounding peat using a knife and were 24–28 cm long and 10 × 10 cm in diameter. The other cores were collected with an Eijelkamp 11-cm diameter circular push corer. ^{210}Pb was analyzed in six cores collected in 2013 and in four cores collected in 2014. The remaining cores were collected in 2011 and 2012 and were analyzed for ^{14}C. The cores from 2011-2014 were subsampled discontinuously, mostly in 4 cm intervals: 1–5 cm, 5–9 cm, 10–14 cm, 20–24 cm, 30–34 cm, 40–44 cm, etc., down to a maximum of 80–84 cm.

Porewater for DIC analysis was collected in the field prior to coring, using syringes attached to stainless steel tubes with holes in the lower 3 cm. Porewater was filtered through GF/D filters into borosilicate 30 mL preweighed vials that had been evacuated and sealed with butyl rubber stoppers. Fifteen to twenty mL of pore water was injected into the vials and they were acidified with 0.3 mL of 20% H_3PO_4.

2.3. Automatic Chamber Measurements

Carbon dioxide and CH_4 gas fluxes were measured with automatic chambers that were placed within each site (three each at the palsa, bog, and fen). The chambers are static, closed systems and have been described in Bäckstrand et al. (2008). The Bäckstrand study chambers were replaced in 2012 with larger chambers (0.178 m^2 basal area) as described in Bubier et al. (2003). Gas concentrations in chamber headspace were measured with a Los Gatos Research (LGR) Fast Greenhouse Gas Analyzer from 2012 through 2018. Sampling was done every 3 hr, and the chamber was closed for 5–8 min for each measurement. Timing control and data acquisition was done with a Campbell CR10x. The chambers failed to record reliable CH_4 flux measurements in the palsa, bog, and fen chambers on 491, 513, and 508 days, respectively. CO_2 flux measurements failed on 417, 438, and 431 days for the palsa, bog, and fen chambers, respectively. For days of the year when the chambers failed to record reliable gas fluxes, measurements from the same day of the year in other years were averaged to fill the gaps. For CH_4 there were between 29 and 169 measurements for each daily average used to gap fill and for CO_2 there were between 26 and 167 measurements. Temperatures for the fen were measured every 30 min using CSI T-107 thermistors placed at several depths below and above the peat surface at the InterAct fen tower located ca. 150 m to the northwest of the chambers. For each habitat, we combined mean annual CO_2 and CH_4 fluxes into a $CO_{2\text{-equivalent}}$ flux using the 100-yr GWP value for methane (27.2 ± 11; Forster et al., 2021).

2.4. Analysis of Bulk Density, %C, and DIC

Dry bulk density (BD) was determined from the weight of a known volume of wet sample recovered from the field following oven-drying or freeze-drying. Organic carbon (OC) content was measured after grinding peat to a homogenous powder in a Spex Sampleprep 5100 mixer-mill, then analyzing on a Carlo Erba elemental analyzer following flash combustion. In samples for which BD or organic carbon was not measured, these values were estimated using the average of samples from the same depth and type of habitat (Table S2 in Supporting Information S1). Bulk density and organic carbon content in samples from discrete depths (4 or 5 cm intervals) from palsa and collapsed palsa sites, bog sites, and fen sites were averaged and assumed to represent the BD or OC in samples from the same habitat type and depth range when there were no direct measurements of these values in the sample.

Upon return to the lab, vials containing filtered porewater were brought to gauge pressure by injecting helium, and $\delta^{13}C$ and concentrations of the DIC were determined by injecting 250 microliters of the headspace gas into a Hewlett Packard gas chromatograph coupled to a Thermo Finnigan Delta V Isotope ratio mass spectrometer. NBS-19 was used as a working standard and results are reported relative to V-PDB. For ^{14}C analysis, vials were subsequently stripped of CO_2 in a Helium stream and the resulting CO_2 purified by vacuum distillation. CO_2 was sealed into breakseals and analyzed at the National Ocean Sciences Accelerator Mass Spectrometry (AMS) facility (NOSAMS) at Woods Hole Oceanographic Institute.

2.5. Radioisotope Analysis

Alpha spectrometry was used to indirectly determine the activity of ^{210}Pb by measuring its decay product, ^{210}Po ($t½ = 138.4$ d), assuming secular equilibrium with this relatively short-lived radioisotope. The chemical process and self-plating of polonium onto silver discs follows methods described in detail elsewhere (Ebaid & Khater, 2006; Flynn, 1968; Martin & Rice, 1981). After plating, the discs were removed, rinsed with de-ionized water, and allowed to air dry. Activities of the internal tracer ^{209}Po together with ^{210}Po on the discs were counted in one of eight silicon semiconductor detectors in an Ortec Octete alpha spectrometer. Uncertainties were estimated using standard counting statistics.

The ^{14}C in bulk peat from selected depths in palsa, collapsed palsa, bog, and fen cores was measured at NOSAMS (Corbett et al., 2013). Peat samples were combusted to CO_2 at Florida State University in quartz tubes at 850°C and then converted to graphite targets and analyzed by AMS (Vogel et al., 1984). Values of ^{14}C are reported according to the standard Δ notation that normalizes the ^{14}C content of a sample to a nominal $\delta^{13}C$ value (−25‰) and collection time (Stuiver & Polach, 1977). The ^{14}C and ^{210}Pb data are available in Table S2 in Supporting Information S1.

2.6. ^{210}Pb- and ^{14}C-Derived Ages and Accumulation Rates

Continuous peat ages in 1 cm increments were obtained from ^{14}C and total ^{210}Pb activity using the Plum and Bacon age-depth models in R version 4.1.1 (Aquino-Lopez et al., 2018; Blaauw & Christen, 2011; R Core Team, 2021). The Plum model uses Bayesian analysis of ^{210}Pb activity alone, or in combination with ^{14}C, to provide robust age estimates even in discontinuously sampled cores. For cores in which only ^{14}C measurements were available, the Bacon age-depth model was used to estimate peat ages. The ^{14}C calibration curves used were IntCal20 and NH1 (Hua et al., 2013; Reimer et al., 2020). Radiocarbon ages and errors for input to Plum and Bacon were calculated from the fraction modern (Fm) measurements using the function pMC.age in R. The measured total ^{210}Pb activity and Fm ^{14}C values that were input to Plum and Bacon are shown in Table S2 in Supporting Information S1. The resulting age-depth models are shown in Figure S1 in Supporting Information S1.

Carbon accumulation was estimated for whole cores by dividing the age of the deepest peat section by the total carbon stock in the core. This is the long-term carbon accumulation rate (LORCA). To observe temporal variations in carbon accumulation, apparent carbon accumulation rates (aCAR) were calculated from the modeled ages at each cm of peat using Equation 1.

$$\text{aCAR} = (\text{OC\%} * \text{BD} * \text{Depth\_Interval})/\text{Age\_Duration} \quad (1)$$

The "Depth Interval" in Equation 1 is always 1 cm and "Age Duration" is the span of years that a given cm of peat accumulated (modeled age of each 1 cm peat section less the age of the section above). The activity of ^{210}Pb that is not from atmospheric fallout and is instead supplied from ^{226}Ra in the soil is "supported" ^{210}Pb and this value is needed to determine total inventory of excess ^{210}Pb, which is used for dating. Core S-1 2016 was not long enough to reach the levels where excess ^{210}Pb was not present (Figure S2 in Supporting Information S1). Because the other four bog cores did reach levels of only supported ^{210}Pb activity, we used the average of these levels to represent supported ^{210}Pb in S-1 2016, since all the bog cores are from the same area and site type.

In addition to LORCA, we calculated aCAR for 3 time periods: recent (1990 to between 2011 and 2016, which is when the cores were retrieved), multi-decadal (1850–1990), and millennial (200–4,500 years BP) by averaging the aCARs for each 1 cm peat interval from each of the three time periods.

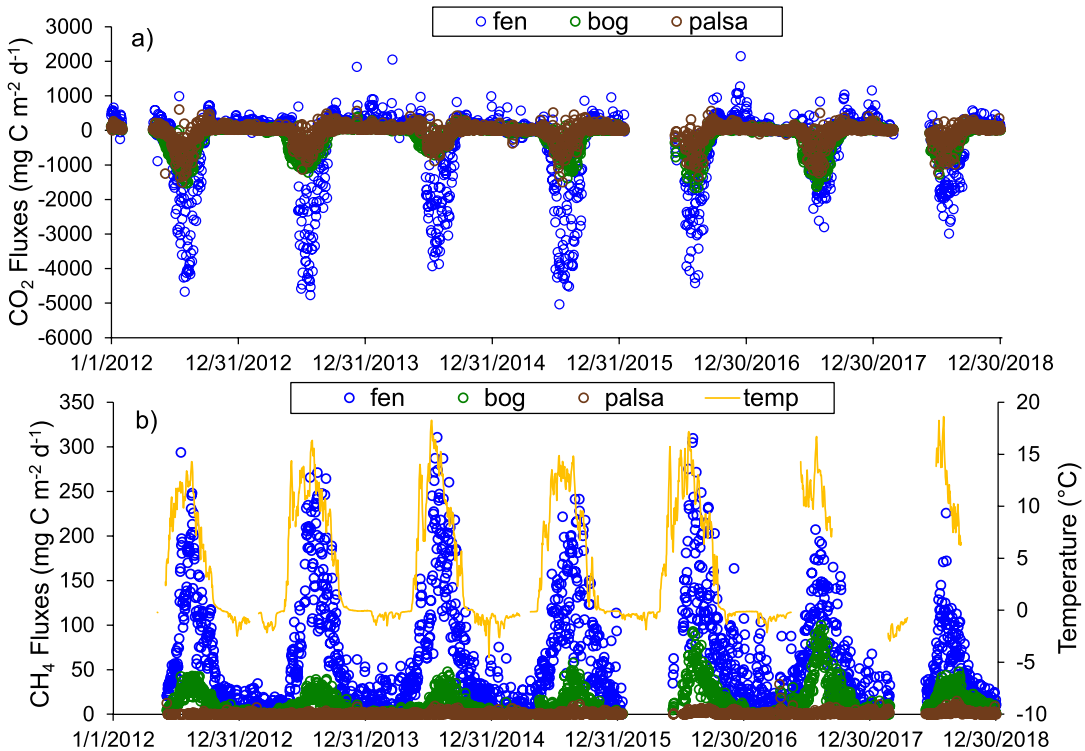

Figure 2. (a) Carbon dioxide and (b) CH_4 fluxes from the palsa (brown circles), bog (green circles), and fen (blue circles) autochamber sites. Fluxes are daily averages of several (up to $n = 24$) measurements per day. Negative numbers indicate fluxes into the peatland and positive numbers represent C losses to the atmosphere. Temperatures (yellow line; daily averages of half-hourly measurements) were measured at the fen 10 cm below the peat surface using CSI T-107 thermistors.

3. Results

3.1. Current C Gas Fluxes

There was net annual CO_2 uptake by the peatland at all sites from 2012 to 2018 (Figure 2a). Median (IQR) CO_2 uptake from June to September was lowest in the palsa, at 162 (−16 to 431) mg C m^{-2} d^{-1}, highest in the fen, at 1,024 (231–2,057) mg C m^{-2} d^{-1}, and bog CO_2 median uptake was 481 (188–778) mg C m^{-2} d^{-1}. From October to May, all sites exhibited net CO_2 efflux: median was 48 (17–97); 37 (10–67); 140 (62–231) mg C m^{-2} d^{-1} in the palsa, bog, and fen, respectively. Methane emissions (Figure 2b) were highest in the fen from June to September with a median of 108 (66–158) mg C m^{-2} d^{-1}. In the bog, median CH_4 production was 22 (12–35) mg C m^{-2} d^{-1} and median C release as CH_4 from the palsa was <1 (0–2) mg C m^{-2} d^{-1}. From October to May, CH_4 was emitted from all three sites, but was near 0 in the palsa, 2 (0–6) mg C m^{-2} d^{-1} in bog peat, and 17 (6–34) mg C m^{-2} d^{-1} at the fen. Temperature at 10 cm below the peat surface was positively correlated with fen CH_4 emissions ($r^2 = 0.64$).

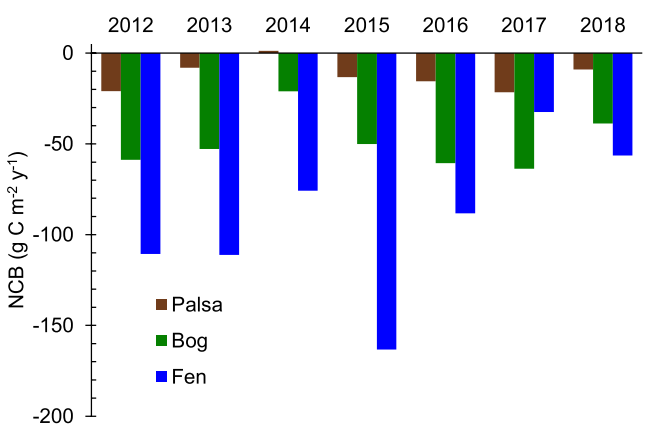

Figure 3. Annual net carbon gas balance was calculated by summing the daily CH_4 for each year and subtracting that from the sum of the daily CO_2 flux for each year. Positive numbers indicate gas fluxes emitted by the peatland into the atmosphere and negative numbers are fluxes into the peatland.

Net carbon gas balance (NCB) is the difference between C uptake by a system through photosynthesis, and its loss to the atmosphere through respiration or gaseous hydrocarbon (such as CH_4) emissions. Annual sums of NCB confirm that all sites, with the exception in 2014 of the palsa, are C sinks (Figure 3). Average annual NCB between 2012 and 2018 increased across the thaw gradient from palsa to bog to fen (−12.5 ± 8.0, −49.4 ± 15.0, and −91.2 ± 42.6 g C m^{-2} y^{-1}) (Table 1). In terms of annual $CO_{2\text{-eq.}}$ flux, the palsa and bog were weak net sinks, while the fen was a net $CO_{2\text{-eq.}}$ source due to higher CH_4 emissions (Table 1).

Table 1
Average Annual CO_2 Flux, CH_4 Flux, Net C Balance, and $CO_{2\text{-equivalent}}$ Flux, All in g C m^{-2} y^{-1}, From 2012 to 2018

	CO_2	s.d.	CH_4	s.d.	NCB	s.d.	$CO_{2\text{-eq.}}$ [a]	s.d.
Palsa	−12.8	8.0	0.3	0.2	−12.5	8.0	−9.8	8.2
Bog	−53.3	15.8	3.9	1.3	−49.4	15.0	−14.7	16.0
Fen	−110.4	44.5	19.2	3.7	−91.2	42.6	79.5	44.7

[a] $CO_{2\text{-eq}}$-C = [44/12*CO_2-C + 16/12*CH_4-C *GWP_100_{CH4}] * 12/44; CO_2 equivalent-C using CH_4 100-yr GWP of 27.2 ± 11 (Forster et al., 2021).

3.2. ^{210}Pb, ^{14}C, and aCAR Across the Thaw Gradient

Basal ages for the bottom of each peat profile were estimated from the age-depth models (Figure 4, Table 2). Six cores with basal ages >1,000 cal BP were between 43 and 95 cm long. The oldest basal ages (>4,000 cal BP) were from two palsa cores (at 95 cm) and one fen core (73 cm). The deepest datable depths of the remaining cores were between 14 and 43 cm deep (some ^{210}Pb-dated cores were longer than the lengths given in Table 2, but excess ^{210}Pb activity was undetectable at these depths in some cases). In cores that were at least 600 years old at the bottom, LORCA was 15–18 g C m^{-2} y^{-1} in palsa/collapsed palsa, 13–23 g C m^{-2} y^{-1} in the bog, and 11–16 g C m^{-2} y^{-1} in fen cores. From 4,460 cal BP until around 1,000 years ago, aCAR was low. It was elevated between 1,000 and 500 years ago and further increased in the past few decades (Figure 5).

LORCAs, calculated from whole cores vary depending, in part, on the length of the core. To compare accumulation rates of discrete time periods, we calculated recent aCAR (from 1990 to between the tops of the cores, or between 2011 and 2016), from 1850 to 1990 (multi-decadal), and pre-1850 (millennial). Recent bog aCAR (147 g C m^{-2} $y^{-1;}$ s.d. = 40) was higher than in the palsa (95 g C m^{-2} $y^{-1;}$ s.d. = 45) or the fen (90 g C m^{-2} $y^{-1;}$ s.d. = 47). Multi-decadal aCAR was lower (72–81 g C m^{-2} $y^{-1;}$ s.d. = 27 to 44) at the three sites and millennial aCAR ranged from 17 to 29 g C m^{-2} $y^{-1;}$ (s.d. = 8 to 28). There was little difference among the sites on the longer timescales (Figure 6).

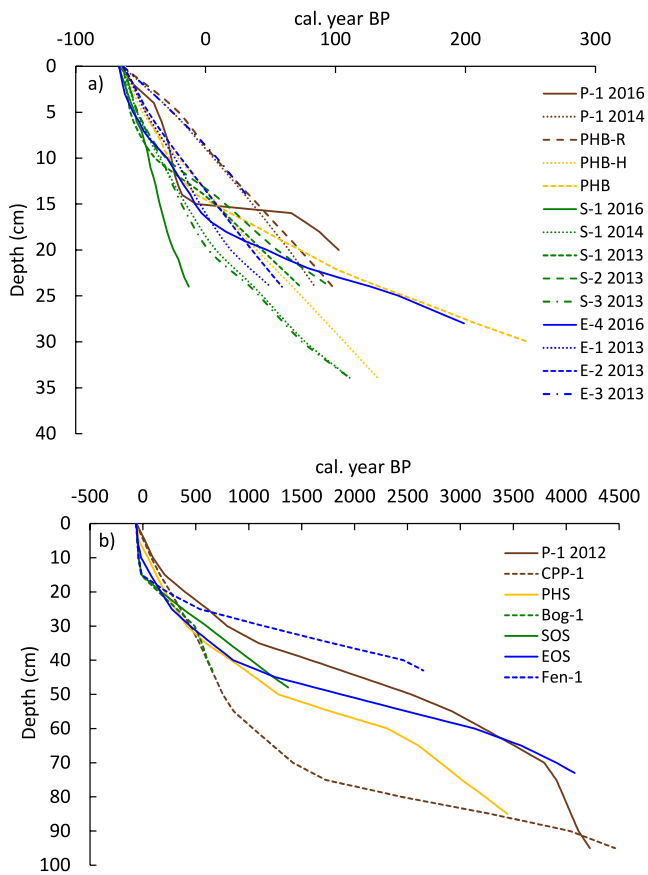

Figure 4. Mean age-depth profiles from the 21 cores analyzed for ^{210}Pb- and ^{14}C-derived ages and modeled with the Plum and Bacon programs in cores with bottom ages (a) <300 years BP and (b) >500 years BP. Brown = palsa, gold = collapsed palsa, green = bog, blue = fen.

Recent and multi-decadal aCARs from all cores were combined in a LOESS (locally weighted polynomial regression) plot to compare differences between sites (Figure 7). We combined palsa and collapsed palsa aCARs for this figure because these are the three habitat types where our autochambers were located. The aCAR values for individual cores used to make the LOESS graph are shown in Figure S3 in Supporting Information S1.

Peat and DIC Δ^{14}C values were similar in palsa, collapsed palsa, and bog sites (Figures 8a and 8b) but DIC values diverged to be more modern than peat values below 30 cm in the fen (Figure 8c). When Δ^{14}C values are greater than 0, this indicates that the peat or DIC is modern (deposited since 1950). The Δ^{14}C peaks at 10 cm in the palsa and fen peat and the less pronounced peak in the bog at around 20 cm represent the ^{14}C pulse from nuclear bomb testing, which peaked around 1963. The Δ^{14}C values of DIC, shown by open symbols in Figure 8, were significantly enriched in fen samples below 30 cm relative to DIC in collapsed palsa. The enriched porewater DIC Δ^{14}C in the fen, relative to the peat for a given depth, indicates that microbial respiration in the fen was dominated either by surface DIC production, or downward transport of surface/young DOC which is respired at depth. This implies that advection brings more modern C to those deeper depths up to at least 80 cm deep in the fen peat profile. In the collapsed palsa (Figure 8a), the ^{14}C of DIC produced by respiration appeared to be more similar to the peat at any depth, suggesting that respiration in the palsa is being supported by the peat at any given depth. In the bog, DIC was similar to the peat at all depths, but was modern.

4. Discussion

4.1. Increasing CH_4 Emissions and CO_2 Uptake Across the Thaw Gradient

Autochamber CH_4 and CO_2 fluxes in Stordalen Mire follow the inundation and thaw gradients, with lowest CH_4 emissions and CO_2 uptake from the palsa, and highest from the fen sites (Figures 2 and 3, Table 1). In Stordalen

Table 2
Long-Term Carbon Accumulation Rates

	Bottom of deepest dated section (cm)	Age at bottom (cal BP)	aCAR (g C m^{-2} y^{-1})	±[a]
Palsa and collapsed palsa				
P-1 2012	95	4,223	15.5	1.0
CPP1	95	4,460	15.4	1.2
PHS	85	3,444	18.4	0.8
PHB	30	248	60.1	27.9
P-1 2016	20	103	27.4	4.9
P-1 2014	24	84	108.3	23.0
PHB-R	24	98	79.8	14.5
PHB-H	34	133	117.6	18.2
Bog				
SOS 2011	48	1,373	13.3	1.0
Bog-1 2012	43	658	23.4	2.5
S-1 2016	24	−13	112.3	22.6
S-1 2014	34	112	75.5	11.5
S-1 2013	24	73	78.3	15.7
S-2 2013	24	96	58.5	12.0
S-3 2013	34	112	75.9	14.7
Fen				
EOS 2012	73	4,080	15.9	0.8
Fen-1 2012	43	2,649	10.9	0.9
E-4 2016	26	166	49.5	12.2
E-1 2013	24	50	88.3	21.3
E-2 2013	24	59	84.0	20.8
E-3 2013	14	31	50.2	13.8

[a]½ of the difference between aCAR calculated from the minimum and maximum ages given by Plum or Bacon age models.

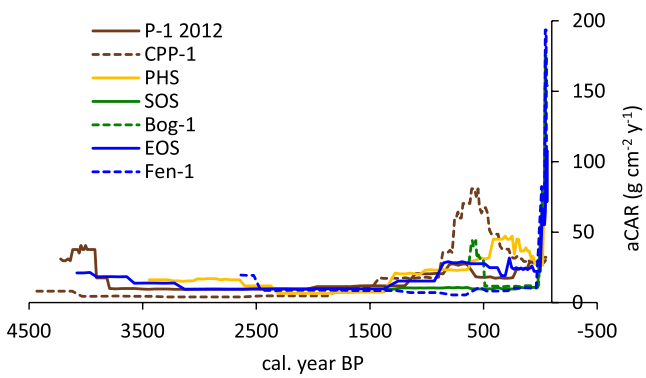

Figure 5. Apparent C accumulation derived from ^{14}C-derived ages in sampled intervals in cores in which the age at the bottom was at least 600 years. Brown = palsa, gold = collapsed palsa, green = bog, blue = fen.

Mire, thawing permafrost resulting in increased water inundation and habitat transition, results in the system becoming a stronger C sink accompanied by increased methane emissions. Our observed 2012–2018 trend of increasing C uptake across the landscape gradient (from NCB of −12.5 (±8.0) g C m^{-2} y^{-1} in palsa to −49.4 (±15.0) g C m^{-2} y^{-1} in the bog, to −91.2 (±42.6) g C m^{-2} y^{-1} in the fen) falls within the NCB estimated by several micrometeorological studies conducted at the site (Table 3). The range of our fen values are consistent with Christensen et al. (2012) who, with micrometeorological techniques that had a footprint encompassing about 83% fen, determined that the mire was a carbon sink at the rate of −46 g C m^{-2} y^{-1}. Johansson et al. (2006) found C uptake rates of −97 g C m^{-2} y^{-1} for fen areas, −73 g C m^{-2} y^{-1} for bog, and −7 g C m^{-2} y^{-1} for palsa over the growing season using automated chambers. Olefeldt et al. (2012) determined NCB in Stordalen Mire to be −46 g C m^{-2} y^{-1} using eddy covariance measurements with a footprint that was about 57% hummock (what we consider palsa) and 43% semiwet areas (bog), similar to the net annual C exchange of −45 g C m^{-2} y^{-1} obtained by Jammet et al. (2017), who also used eddy covariance measurements. The net C uptake we measured was higher than the values of Bäckstrand et al. (2010) who used automated chambers to determine NCB of 30, −29, and −3.1 g C m^{-2} y^{-1} for palsa, bog, and fen, respectively. Our fluxes may differ from those of Bäckstrand et al. (2010) because their data were collected with smaller chambers and contain fewer snow season measurements, with more shoulder season measurements used to represent winter fluxes, likely causing them to overestimate winter CO_2 effluxes. As discussed by Natali et al. (2011), annual flux balances are sensitive to winter emissions, highlighting the importance of our winter measurements. The deviations in NCB between our chamber measurements and these other studies are due to differences in measured CO_2 uptake, that is, the CH_4 fluxes are mostly similar. Our CH_4 fluxes in the palsa and bog (0.3 and 3.9 g C m^{-2} y^{-1}, respectively) were comparable to those of Bäckstrand et al. (2010), who reported values of 0.5, 6.2, and 31.8 g C m^{-2} y^{-1} in palsa, bog, and fen, respectively. Our fen CH_4 flux (19.2 g C m^{-2} y^{-1}) was lower than theirs, but nearly identical to that reported by Jammet et al. (2017) of 21.2 g C m^{-2} y^{-1} and Christensen et al. (2012), who reported CH_4 emission rates of 20 g C m^{-2} y^{-1} for a tower footprint that was 83% fen. Methodologies, footprints, and inter-annual variability likely explain the differences noted between studies. Gas flux rates can also change rapidly, as reported by Svensson et al. (1999), who attributed an increase in CO_2 fluxes from 1974 to 1995 to altered vegetation, mineralization pathways, and permafrost loss. CO_2 uptake and NCB is highest in the fen, but because of the increased CH_4 emissions, the CO_2-equivalent flux is also highest in this habitat. The CO_2-equivalent flux will likely increase as temperatures warm and fen areas expand (Varner et al., 2021).

4.2. Peat Chronology Validated Using Combined ^{14}C and ^{210}Pb

We compared the peat ages obtained with the commonly used Constant Rate of Supply (CRS) calculations, that are based on excess ^{210}Pb activity, with those given by the Plum model using ^{210}Pb in combination with ^{14}C dates. In the three cores for which both ^{210}Pb and ^{14}C measurements were made, the ages were in agreement between the two approaches, except in the 2016 palsa core. There is an increase in age of about 70 years between depths 15 and 16 cm in the 2016 palsa core which is not seen when ^{210}Pb ages are modeled without ^{14}C. This discrepancy may be due to smearing of the ^{14}C chronology

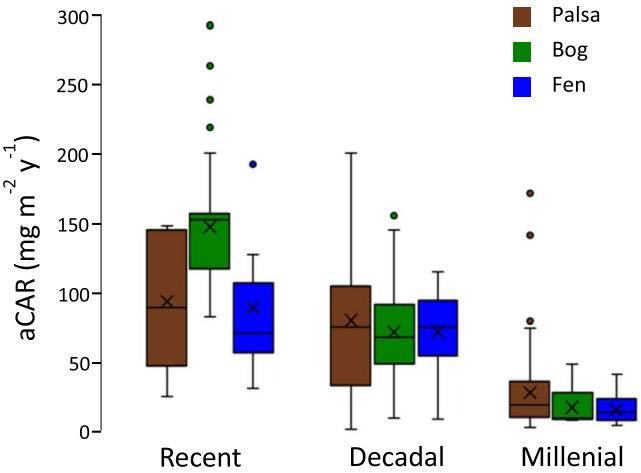

Figure 6. ACAR from the recent past (1990–2016), 1850 to 1990 (multi-decadal), and from more than 4,000 years BP to 1850 (millennial) in palsa, bog, and fen cores.

because of contamination with post-bomb carbon (Goslar et al., 2005). The presence of root material could also make the peat seem younger, but it is unlikely that this would influence the palsa peat more than the fen or bog. Oldfield et al. (1979) presented evidence that downward mobility of ^{210}Pb led to discrepancies between the ^{210}Pb and the pollen ages determined for the ombrotrophic peat they studied. Migration of ^{210}Pb could result in younger ages in deep peat, but this is the opposite of what is seen in the palsa where Plum ages that include ^{14}C are younger in the 4–15 cm interval than when only ^{210}Pb activity is used. Urban et al. (1990) showed that most of their ^{210}Pb inventory in North American peatlands was above the water table in hummocks and below it in the hollows, and more ^{210}Pb was lost from the hollows, where the water table was high. The water table in bogs at Stordalen was 7–30 cm below the surface in the summer and in fens was at or above the surface. From the good agreement between Plum ^{14}C- and ^{210}Pb-derived ages with ^{210}Pb-only ages (CRS method) in the fen core, the higher water table in the fen appears not to have facilitated downward diffusion of ^{210}Pb. The absence of bias to younger ^{210}Pb ages in the three 2016 cores supports the validity of ^{210}Pb-derived ages alone in the cores where ^{14}C measurements are not available.

Loss of ^{210}Pb due to lateral export has the potential to affect the calculated age. Olefeldt and Roulet (2012) found that there was water flow through two fens in the Stordalen peatland complex. Inventories of ^{210}Pb in the peat can provide clues to the possible leaching of ^{210}Pb from the peat. The atmospheric flux is related to the integrated ^{210}Pb activity in the peat by $\phi = \lambda A$, where λ is the decay constant for ^{210}Pb (0.03114 years^{-1}) and A is the total excess ^{210}Pb inventory integrated over the entire core (Appleby & Oldfield, 1992; Preiss et al., 1996). The expected ^{210}Pb inventory based on Baskaran's (2011) atmospheric flux at 68°N of 3.7 ± 3.5 mBq cm^{-2} y^{-1} would be 1,188 ± 1,123 Bq m^{-2} for an entire peat core. Inventories of ^{210}Pb in peat cores taken from Store Mosse, a mire south of Stordalen, were 1,630–2,290 Bq m^{-2} (Olid et al., 2014). The ^{210}Pb inventories for the 2016 bog and fen cores were near this range (1,427 and 1,499 Bq m^{-2}, respectively, Table S3 in Supporting Information S1), indicating that loss of ^{210}Pb is not a factor in these cores. Inventory in the year 2016 palsa core was lower, 836 Bq m^{-2}, which may reflect wind scouring the palsa snowpack (Seppälä, 2003) and depositing it (along with the winter-deposited ^{210}Pb) in lower areas (i.e., bog and fen).

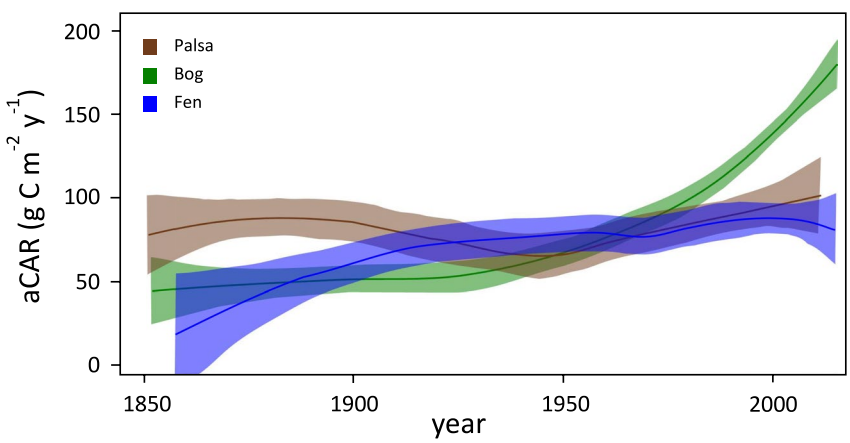

Figure 7. aCAR in palsa and collapsed palsa (brown), bog (green), and fen (blue) sites based on ^{210}Pb and ^{14}C chronology (LOESS, R version 4.1.1). The shaded areas represent the 95% confidence interval and smoothing span = 0.7. Individual profiles are shown in Figure S3 in Supporting Information S1.

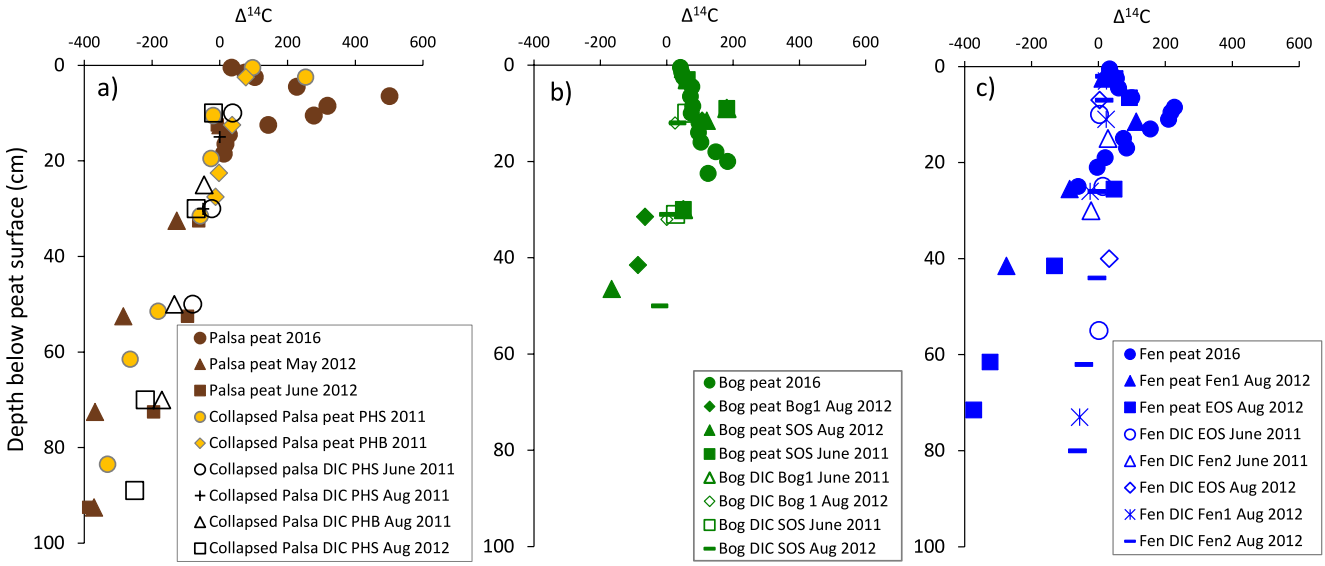

Figure 8. $\Delta^{14}C$ values in dissolved inorganic carbon (DIC) and peat from (a) palsa (brown) and collapsed palsa (gold), (b) bog (green), and (c) fen (blue) sites. Filled symbols represent peat $\Delta^{14}C$ values and open symbols and crosses indicate DIC $\Delta^{14}C$ values. The profiles show $\Delta^{14}C$ values from several cores at each site (the high-resolution cores from 2016, some of the low-resolution cores discussed in the text, and additional low-resolution cores from 2011 and 2012). Analytical precision of $\Delta^{14}C$ was <±7.2‰.

4.3. Carbon Accumulation Rates Reflect Degree of Decomposition and Productivity

The low millennial aCAR in all three site types (29 ± 28, 18 ± 13, and 17 ± 8 g C m^{-2} y^{-1} in the palsa, bog, and fen, respectively; Figure 9) is similar to those of a pan-Arctic compilation by Treat et al. (2016), who found long-term (>1,000 year) C accumulation of 14 g C m^{-2} y^{-1} in permafrost peatlands 18 g C m^{-2} y^{-1} in permafrost-free bogs, and 23 g C m^{-2} y^{-1} in fens. The trend of increasing aCAR from longer (millennial) to shorter (multi-decadal and recent) timescales seen in all three of our habitat types (Figure 9) was noted by Olid et al. (2020) in a permafrost plateau near Stordalen Mire. They reported C accumulation rates of <20 g C m^{-2} y^{-1} at millennial time scales, ~40 g C m^{-2} y^{-1} at the multi-decadal scale and >80 g C m^{-2} y^{-1} in recent peat. Kokfelt et al. (2010) reported carbon accumulation rates of 18–51 g C m^{-2} y^{-1} at a bog-like site in Stordalen Mire. Sampling from

Table 3
Compilation of Literature Values for C Uptake and Emission at Stordalen Mire

Site	CO_2 (g m^{-2} y^{-1})	CH_4 (g m^{-2} y^{-1})	Net (g m^{-2} y^{-1})	Method	Source
Palsa	−12.8 (−22–1)	0.3 (0.12–0.59)	−12.5	Autochamber	This study
Bog	−53.3 (−70–−24)	3.9 (2.8–6.0)	−49.4	Autochamber	This study
Fen	−110.4 (−184–−49)	19.2 (12.4–23)	−91.2	Autochamber	This study
Hummock (~palsa)	−6.7	−0.1	−6.8	Autochamber	Johansson et al. (2006)
Semiwet + wet (~bog)	−73	19.1	−53.9	Autochamber	Johansson et al. (2006)
Tall graminoid (~fen)	−97.4	33	−64.4	Autochamber	Johansson et al. (2006)
Palsa	29.7 (9[a])	0.5 (5[a])	30.2 (11[a])	Autochamber	Bäckstrand et al. (2010)
Sphagnum-site (~bog)	−35.3 (3[a])	6.2 (1[a])	−29.1 (4[a])	Autochamber	Bäckstrand et al. (2010)
Eriophorum-site (~fen)	−34.9 (4[a])	31.8 (1[a])	−3.1 (5[a])	Autochamber	Bäckstrand et al. (2010)
Fen	−66.3 (3[b])	21.2 (1.3[b])	−45.1	Eddy covariance	Jammett et al. (2017)
83% fen	−66 (−95 to −20)	20 (18–22)	−46 (−73–0)	Eddy covariance	Christensen et al. (2012)
57% hummock (~palsa), 43% semiwet (~bog)			−46 (−56–−33)	Eddy covariance	Olefeldt et al. (2012)

Note. Numbers in parentheses are ranges.
[a]Coefficient of variation. [b]Standard deviation.

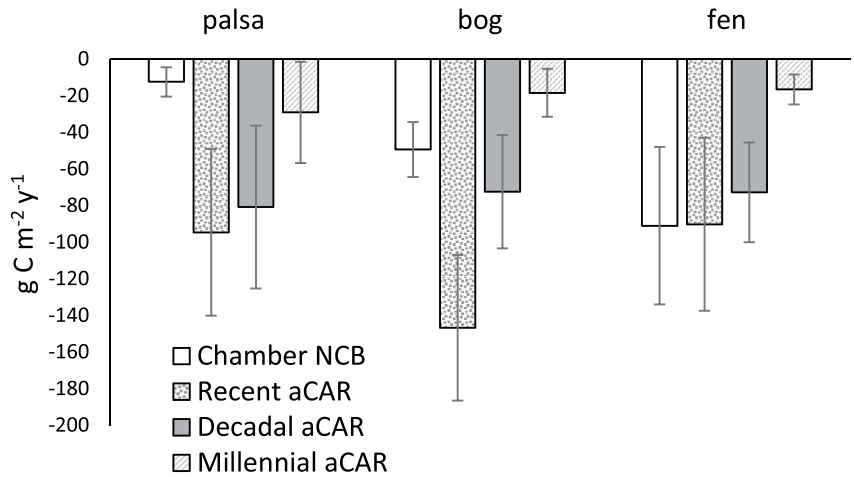

Figure 9. Apparent carbon accumulation (aCAR) across the thaw gradient measured at four timescales. Chamber net carbon gas balance (NCB) from 2012 to 2018 is represented by open bars. Recent (1990 to 2011–2016), multi-decadal (1850–1990), and millennial (200–4,500 years) aCARs are plotted as negative values to be comparable with NCB. Error bars are standard deviation. Palsa aCAR includes collapsed palsa.

another location in Stordalen Mire, Sim et al. (2021) report low carbon accumulation rates (<10 g C m^{-2} y^{-1}) for a palsa core and ~10–50 g C m^{-2} y^{-1} for a bog core prior to 300–400 BP. In our data, carbon accumulation was higher across the mire during the last ~150 years relative to the centuries and millennia prior (Figures 6 and 9). This was also the case for the bog core (aCAR > 100 g C m^{-2} y^{-1}) analyzed by Sim et al. (2021), while their palsa core had aCAR ~60 g C m^{-2} y^{-1} for a few hundred years before dropping to lower rates recently. aCAR rose further in the last 25 years, in the bog and palsa, but this rise is not observed in the fen. These apparent increases in recent rates must be viewed with caution as discussed by Young et al. (2019), who noted that surface peat layers may be offset with regard to the timing between organic matter production and decomposition. That is, surface layers can still have fresh organic matter inputs from roots and have had less time to lose organic matter through decomposition, while deeper layers below the depth of excess ^{210}Pb are dominated by continuing decomposition.

Recent aCAR (post 1990) was higher than indicated by autochamber NCB (except at the fen) (Figure 9). The discrepancy between NCB and recent aCAR may be explained because NCB captures C flux from the entire peat column and recent aCAR is the C accumulation only in the upper 20–30 cm. If the accumulated NCB could be integrated over the whole peat core and aCAR of the entire core (to the lowest layer of peat) could be accurately estimated using the basal ^{14}C date, for example, these measures should be equal, but over shorter time scales NCB and aCAR can differ (Frolking et al., 2014; Young et al., 2019). We expect the largest component of the flux measured by the chambers to originate near the surface, and that flux is highly influenced by local weather conditions. Decomposition occurs mainly in the acrotelm (the surface peat layer with a fluctuating water table, experiencing occasional to frequent oxic conditions, and living plant roots), but also proceeds in the catotelm (deeper peat that is perennially saturated and generally anoxic), albeit more slowly (Clymo, 1984). Incubation of peat from Stordalen Mire shows that CO_2 production occurs in incubated fen and bog peat from at least as deep as 25–35 cm depth and likely below that depth (Wilson et al., 2019; Wilson, Zayed, et al., 2021). If decomposition is happening deep in the peat profile at the same time that there is high productivity at the top of the peat, the net CO_2 flux that the chambers record would be lower than the accumulation rate estimated by recent aCAR, which measures accumulation near the surface and misses the decomposition of material below. In this case, the high CO_2 influx into surface peat could be offset by the CO_2 being emitted below, causing lower CO_2 fluxes measured by chambers as compared to ^{210}Pb accumulation rate (e.g., Heffernan et al., 2020; Jones et al., 2013; O'Donnell et al., 2012; Young et al., 2019). Wilson et al. (2017) also found higher C accumulation rates in peat measured by ^{210}Pb compared to chamber fluxes in Alberta, Canada.

Time scales between surface carbon uptake and subsequent respiration of that carbon may be more depth dependent in the bog than in the fen. The differences between recent aCAR and NCB in both the bog and palsa relative to the fen (Figure 9) may be attributed to *Sphagnum* and shrub litter recalcitrance (Verhoeven & Liefveld, 1997). Although tall graminoids (i.e., *Eriophorum* spp.), which are the dominant vegetation in the fen, have a higher

initial C sequestration rate than sphagnum hummocks and shrubs (Figures 2 and 3), the graminoid litter is more degradable (Hodgkins et al., 2014). Hodgkins et al. (2016) reported that peat and dissolved organic matter became more labile across the thaw gradient in Stordalen Mire, based on peat humification indices. More evidence comes from Fourier transform infrared (FT-IR) results, which show that organic matter in fen peat decomposes sooner after deposition than in the bog (R. Wilson, personal communication, 2021). Similarly, three-fold higher carbon litter input to graminoid sites (fen) relative to a moss hummock (bog) have been reported (Malmer & Wallén, 1996; Malmer et al., 2005). But ^{14}C-labeling showed that when decomposition was considered, input to the catotelm in fens was only -9 g C m^{-2} y^{-1} compared with moss hummocks, semiwet, and wet sites (-22 to -26 g C m^{-2} y^{-1}), which we take to be equivalent to bogs (Malmer et al., 2005). Thus, the time (and depth) between surface layer fixation and subsequent respiration of that carbon appears less pronounced in the fen, where the organic matter reactivity is apparently greater and decomposes on a faster time scale. Export of DOC, which occurs at a higher rate in fens at Stordalen than bog or palsa peat (Olefeldt & Roulet, 2012), may contribute to reduced aCAR at the fen. Olefeldt and Roulet (2012) found that two to three times more DOC was exported from fen habitats than from bog and palsa, but the amount lost was 6.8 g C m^{-2} y^{-1}, which is about 7% of fen NCB.

The Δ^{14}C in deep collapsed palsa DIC, representing the products of microbial respiration and production of both CO_2 and CH_4 (Chanton et al., 2008), is depleted in ^{14}C. The palsa peat is also ^{14}C-depleted, pointing to decomposition of the deep peat as the source of the DIC (Figure 8). This pattern indicates that some portion of the deeper palsa peat is labile and decomposable. In the palsa, the active layer is deeper than the penetration by ^{210}Pb, and inevitably, decomposition is occurring below the ^{210}Pb profile. In the bog, we only have Δ^{14}C measurements in DIC from above 50 cm depth, so it is unknown whether respiration of deep, old C is occurring below that depth. The Δ^{14}C of DIC was enriched in fen samples relative to DIC in collapsed palsa, indicating the respiration of recently fixed C dominated microbial respiration in the fen system, which has high surface and root primary production. In the fully thawed fen habitat, Δ^{14}C-enriched respiration products (DIC) penetrated the subsurface to depths of 80 cm (Figure 8), consistent with deep roots of sedges (Saarinen, 1996). The DIC in neither the bog nor fen cores reflected 50+ year old bomb carbon but was always consistent with more recent surface production. Because microbial respiration in the surface of these wetlands was dominated by the input of modern substrates, so too would be the CH_4 emitted from these sites (Chanton et al., 2008).

The extent of decomposition of catotelm peat underlying the acrotelm has been the subject of a number of investigations, but a clear pattern has not emerged. Ratcliffe et al. (2018) investigated a blanket bog in Scotland and found that net ecosystem exchange as measured by eddy covariance was six times greater than LORCA of C measured by ^{14}C dating. Ratcliffe et al. (2018) point out that long-term accumulation depends on the transfer of organics from the acrotelm to the catotelm, the rate of which is variable and dependent on a number of factors including litter quality and turnover, and water table position. Ratcliffe et al. (2018) note that inclusion of the acrotelm peat in estimates of long-term accumulation may cause overestimate of accumulation as the younger surface peats have undergone less decomposition. Pelletier et al. (2017) argued that long-term accumulation at silvic peat plateaus was similar to adjacent permafrost thaw areas because higher deep peat degradation rates in thawed areas compensated for increased surface carbon uptake that occurred upon thaw, inundation, and the transformation of the permafrost plateau to a wetland bog. Long-term accumulation was similar in the plateau (17.7 g C m^{-2} y^{-1}) and the bog (20.6 g C m^{-2} y^{-1}). O'Donnell et al. (2012) made a series of measurements along a chronosequence in Alaska. They found that about 50% more carbon was stored in permafrost plateaus relative to bogs resulting from thaw. They also observed a temporal offset between carbon accumulation and decomposition. Initially upon thaw, they noted rapid accumulation in near-surface bog peat, which was eventually balanced by increased decomposition of thawed silvic peat in the deeper layers.

In addition to the temporal differences between surface peat production and deep decomposition, the higher aCAR observed in recent years in Stordalen Mire may partly reflect enhanced productivity brought on by rising temperatures or by increased precipitation in the 1980's (Kokfelt et al., 2009). Mean annual temperatures increased 2.5°C from years 1913 to 2006 (Callaghan et al., 2010). Increasing temperatures and longer growing seasons result in greater rates of peat accumulation (Ratcliffe et al., 2018), as evidenced by the rapid expansion of peatlands during the early Holocene warm period (Yu, 2012; Yu et al., 2009). The response of permafrost systems to warming is more complex than the hypothesized large release of carbon (Bouskill et al., 2020; MacDougall et al., 2012; Riley et al., 2021). As discussed by Treat and Frolking (2013), the height of the water table following thaw is a large determinant in the fate of thawed organic matter. In systems that become inundated following

thaw, ecosystem productivity increases by as much as a factor of 2–5 (Camill, 1999; Camill et al., 2001; Jones et al., 2013), but this increased surface carbon sequestration may be balanced by increased respiration of deeper previously frozen material (Jones et al., 2013). Jones et al. (2017) found that upon thaw, C loss of the permafrost peat was about 30% of the initial C stock and that loss of carbon was directly proportional to the pre-thaw C stock. Permafrost areas were net C sources to the atmosphere for a decade following thaw before they returned to net C sinks. The quantity of respiration balancing surface ecosystem production is dependent upon the amount of carbon decomposing, and how reactive it is (Jones et al., 2017; O'Donnell et al., 2012). The reactivity of buried organic matter is partially determined by the extent to which it is inundated (Lee et al., 2012).

We found minimal contribution of thawed aged peat to soil respiration, regardless of whether the thaw had occurred decades or centuries before. This agrees with findings of Heffernan et al. (2020), who reported no long-term impact of permafrost thaw on carbon inventories in a permafrost peatland in western Canada. Increased carbon deposition following thaw was offset by losses of thawed permafrost. Elberling et al. (2013) reported little loss of carbon stocks with thawing over a 12-year period in water saturated peat. Estop-Aragones, Cooper, et al. (2018) and Estop-Aragones, Czimczik, et al. (2018) measured the radiocarbon content of both peat and respired CO_2 in the western Canada discontinuous permafrost zone. With the exception of recent permafrost collapse features, we find that respiration products are dominated by modern production. Estop-Aragones, Cooper, et al. (2018) and Estop-Aragones, Czimczik, et al. (2018) suggested that the greater carbon uptake associated with thaw and the preservation of deeper material under anoxic waterlogged conditions would offset the increased CH_4 emissions accompanying inundation. Cooper et al. (2017) reported similar findings, that aged carbon was not contributing significantly to soil respiration, but that increased CH_4 emissions would dilute the effectiveness of the stronger CO_2 sink that resulted when peat plateaus thawed and became inundated and anaerobic. This finding echoes that of Turetsky et al. (2007) and is in agreement with our work, that is, that the loss of surface permafrost in our peatland increased net carbon storage and increased CH_4 emissions that offset this enhanced peatland carbon sink.

5. Conclusions

The trajectory of permafrost landscape change due to thaw (i.e., palsa to bog to fen) and the timing of that change (i.e., abrupt collapse and inundation vs. gradual hydrologic and subsequent vegetation transition) are difficult to predict and depend on many underlying ecosystem traits. Our results indicate that Stordalen Mire's recent landscape change, with an increase in thawing permafrost causing increased water inundation and habitat transition, results in the system becoming a stronger C sink based upon recent NCB. Across the wetland gradient, increased methane emission accompanying the stronger carbon sink will result in an increased global warming potential of the mire complex with respect to atmospheric forcing. We found minimal contribution of thawed aged peat to soil respiration indicating that methane emissions from this landscape are dominated by modern carbon.

Appendix A

IsoGenie Project Coordinators (those coordinating the IsoGenie Project during the period when this research was primarily accomplished): **S. R. Saleska**, Department of Ecology and Evolutionary Biology, University of Arizona, Tucson, AZ 85716, USA; **V. I. Rich**, Department of Microbiology, The Ohio State University, Columbus, OH 43210, USA, Department of Soil, Water and Environmental Sciences, University of Arizona, Tucson, AZ 85716, USA; **P. M. Crill**, Department of Geological Sciences and Bolin Centre for Climate Research, Stockholm University, 10691 Stockholm, Sweden; **J. P. Chanton**, Department of Earth, Ocean, and Atmospheric Science, Florida State University, Tallahassee, FL 32306, USA; **G. W. Tyson**, Center for Microbiome Research, School of Biomedical Sciences, Queensland University of Technology, Woolloongabba, Queensland 4102, Australia; **R. K. Varner**, Earth Systems Research Center, Institute for the Study of Earth, Oceans and Space, and Department of Earth Sciences, University of New Hampshire, Durham, NH 03824, USA; **M. Sullivan**, Department of Microbiology, The Ohio State University, Columbus, OH 43210, USA; **S. Frolking**, Earth Systems Research Center, Institute for the Study of Earth, Oceans and Space, and Department of Earth Sciences, University of New Hampshire, Durham, NH 03824, USA; **C. Li**, Earth Systems Research Center, Institute for the Study of Earth, Oceans and Space, and Department of Earth Sciences, University of New Hampshire, Durham, NH 03824, USA.

Appendix B

IsoGenie Field Team (those who collected field data and samples during the period when this research was primarily accomplished): **D. Anderson**, Department of Soil, Water and Environmental Sciences, University of Arizona, Tucson, AZ 85716, United States; **S. Dominguez**, Department of Ecology and Evolutionary Biology, University of Arizona, Tucson, AZ 85716, United States; **A. J. Garnello**, Department of Ecology and Evolutionary Biology, University of Arizona, Tucson, AZ 85716, United States; **M. Hough**, Department of Soil, Water and Environmental Sciences, University of Arizona, Tucson, AZ 85716, United States, Department of Ecology and Evolutionary Biology, University of Arizona, Tucson, AZ 85716, United States; **J. Jansen, M. Wik, B. Thornton, E. Nörback**, Department of Geological Sciences and Bolin Centre for Climate Research, Stockholm University, 10691 Stockholm, Sweden; **R. Jones**, Cold Regions Research and Engineering Laboratory, Hanover, NH 03755, USA; **E.-H. Kim**, Department of Soil, Water and Environmental Sciences, University of Arizona, Tucson, AZ 85716, United States; **T. A. Logan, N. Rakos, H. Öste, P. Marklund and R. Holden**, Abisko Scientific Research Station, Swedish Polar Research Secretariat, SE-981 07 Abisko, Sweden; **R. Mondav**, Australian Centre for Ecogenomics, School of Chemistry and Molecular Biosciences, University of Queensland, Brisbane, QLD, Australia; **A. Persson**, Lund University, Department of Biology, Lund, Sweden; **N. Raab**, Department of Microbiology, The Ohio State University, Columbus, OH 43210, USA; **K. Solheim**, Department of Soil, Water and Environmental Sciences, University of Arizona, Tucson, AZ 85716, United States; **G. Trubl**, Department of Soil, Water and Environmental Sciences, University of Arizona, Tucson, AZ 85716, United States; **G. W. Tyson**, Center for Microbiome Research, School of Biomedical Sciences, Queensland University of Technology, Woolloongabba, Queensland 4102, Australia.

Data Availability Statement

Geochemical and gas flux data are available from the Isogenie Database website (https://isogenie-db.asc.ohio-state.edu/datasources#terrestrial_geochem and https://isogenie-db.asc.ohio-state.edu/datasources#fluxes), and peat temperature data from the Swedish Infrastructure for Ecosystems Sciences (SITES) data portal (https://data.fieldsites.se/portal/).

Acknowledgments
The authors thank Samantha Bosman, Brittany Verbeke, and Claire Wilson for assistance in the lab and Abisko Scientific Research Station for sampling infrastructure. We gratefully acknowledge the IsoGenie field team. We would like to acknowledge the following funding in support of this project: Swedish Research Council (Vetenskapsrådet, VR) grants (NT 2007-4547 and NT 2013-5562 to P. Crill), U.S. Department of Energy grants (DE-SC0004632 and DE-SC0010580 to V. Rich and S. Saleska), and U.S. National Science Foundation MacroSystems Biology grant (NSF EF #1241037, PI Varner). This work was supported by the U.S. Department of Energy, Office of Science, Office of Biological and Environmental Research under the Genomic Science program. We thank the reviewers for their thorough reading of the manuscript and whose comments greatly improved the manuscript. We also acknowledge funding from the National Science Foundation for the EMERGE Biology Integration Institute, NSF Award #2022070.

References

Åkerman, H. J., & Johansson, M. (2008). Thawing permafrost and thicker active layers in sub-arctic Sweden. *Permafrost and Periglacial Processes*, *19*(3), 279–292. https://doi.org/10.1002/ppp.626

Appleby, P. G., & Oldfield, F. (1992). Applications of lead-210 to sedimentation studies. In *Uranium-series disequilibrium: Applications to earth, marine, and environmental sciences. 2*.

Aquino-Lopez, M. A., Blaauw, M., Christen, J. A., & Sanderson, N. K. (2018). Bayesian analysis of ^{210}Pb dating. *Journal of Agricultural, Biological, and Environmental Statistics*, *23*(3), 317–333. https://doi.org/10.1007/s13253-018-0328-7

Bäckstrand, K., Crill, P., Jackowicz-Korczyñski, M., Mastepanov, M., Christensen, T., & Bastviken, D. (2010). Annual carbon gas budget for a subarctic peatland, Northern Sweden. *Biogeosciences*, *7*(1), 95–108. https://doi.org/10.5194/bg-7-95-2010

Bäckstrand, K., Crill, P. M., Mastepanov, M., Christensen, T. R., & Bastviken, D. (2008). Non-methane volatile organic compound flux from a subarctic mire in Northern Sweden. *Tellus B: Chemical and Physical Meteorology*, *60*(2), 226–237. https://doi.org/10.1111/j.1600-0889.2007.00331.x

Baskaran, M. (2011). Po-210 and Pb-210 as atmospheric tracers and global atmospheric Pb-210 fallout: A review. *Journal of Environmental Radioactivity*, *102*(5), 500–513. https://doi.org/10.1016/j.jenvrad.2010.10.007

Blaauw, M., & Christen, J. A. (2011). Flexible paleoclimate age-depth models using an autoregressive gamma process. *Bayesian Analysis*, *6*(3), 457–474. https://doi.org/10.1214/ba/1339616472

Bouskill, N. J., Riley, W. J., Zhu, Q., Mekonnen, Z. A., & Grant, R. F. (2020). Alaskan carbon-climate feedbacks will be weaker than inferred from short-term experiments. *Nature Communications*, *11*(1), 5798. https://doi.org/10.1038/s41467-020-19574-3

Bubier, J., Crill, P., Mosedale, A., Frolking, S., Linder, E. (2003). Peatland responses to varying interannual moisture conditions as measured by automatic CO2chambers. *Global Biogeochemical Cycles*, *17*(2). https://doi.org/10.1029/2002gb001946

Burke, S. A., Wik, M., Lang, A., Contosta, A. R., Palace, M., Crill, P. M., & Varner, R. K. (2019). Long-term measurements of methane ebullition from thaw ponds. *Journal of Geophysical Research: Biogeosciences*, *124*(7), 2208–2221. https://doi.org/10.1029/2018jg004786

Callaghan, T. V., Bergholm, F., Christensen, T. R., Jonasson, C., Kokfelt, U., & Johansson, M. (2010). A new climate era in the sub-Arctic: Accelerating climate changes and multiple impacts. *Geophysical Research Letters*, *37*(14), L14705. https://doi.org/10.1029/2009gl042064

Camill, P. (1999). Peat accumulation and succession following permafrost thaw in the boreal peatlands of Manitoba, Canada. *Écoscience*, *6*(4), 592–602. https://doi.org/10.1080/11956860.1999.11682561

Camill, P., Lynch, J. A., Clark, J. S., Adams, J. B., & Jordan, B. (2001). Changes in biomass, aboveground net primary production, and peat accumulation following permafrost thaw in the boreal peatlands of Manitoba, Canada. *Ecosystems*, *4*(5), 461–478. https://doi.org/10.1007/s10021-001-0022-3

Chanton, J., Glaser, P., Chasar, L., Burdige, D. J., Hines, M., Siegel, D., et al. (2008). Radiocarbon evidence for the importance of surface vegetation on fermentation and methanogenesis in contrasting types of boreal peatlands. *Global Biogeochemical Cycles*, *22*(4), GB4022. https://doi.org/10.1029/2008gb003274

Christensen, T. R., Jackowicz-Korczyński, M., Aurela, M., Crill, P. M., Heliasz, M., Mastepanov, M., & Friborg, T. (2012). Monitoring the multi-year carbon balance of a subarctic palsa mire with micrometeorological techniques. *Ambio*, *41*(3), 207–217. https://doi.org/10.1007/s13280-012-0302-5

Christensen, T. R., Johansson, T., Åkerman, H. J., Mastepanov, M., Malmer, N., Friborg, T., et al. (2004). Thawing sub-arctic permafrost: Effects on vegetation and methane emissions. *Geophysical Research Letters*, *31*(4), L04501. https://doi.org/10.1029/2003gl018680

Clymo, R. (1984). The limits to peat bog growth. *Philosophical Transactions of the Royal Society of London B Biological Sciences*, *303*(1117), 605–654.

Cooper, M. D. A., Estop-Aragones, C., Fisher, J. P., Thierry, A., Garnett, M. H., Charman, D. J., et al. (2017). Limited contribution of permafrost carbon to methane release from thawing peatlands. *Nature Climate Change*, *7*(7), 507–511. https://doi.org/10.1038/nclimate3328

Corbett, J. E., Burdige, D. J., Tfaily, M. M., Dial, A. R., Cooper, W. T., Glaser, P. H., & Chanton, J. P. (2013). Surface production fuels deep heterotrophic respiration in northern peatlands. *Global Biogeochemical Cycles*, *27*(4), 1163–1174. https://doi.org/10.1002/2013gb004677

Dorrepaal, E., Toet, S., Van Logtestijn, R. S., Swart, E., Van De Weg, M. J., Callaghan, T. V., & Aerts, R. (2009). Carbon respiration from subsurface peat accelerated by climate warming in the subarctic. *Nature*, *460*(7255), 616–619. https://doi.org/10.1038/nature08216

Ebaid, Y., & Khater, A. (2006). Determination of ^{210}Pb in environmental samples. *Journal of Radioanalytical and Nuclear Chemistry*, *270*(3), 609–619. https://doi.org/10.1007/s10967-006-0470-5

Elberling, B., Michelsen, A., Schadel, C., Schuur, E. A. G., Christiansen, H. H., Berg, L., et al. (2013). Long-term CO_2 production following permafrost thaw. *Nature Climate Change*, *3*(10), 890–894. https://doi.org/10.1038/nclimate1955

Estop-Aragones, C., Cooper, M. D. A., Fisher, J. P., Thierry, A., Garnett, M. H., Charman, D. J., et al. (2018). Limited release of previously-frozen C and increased new peat formation after thaw in permafrost peatlands. *Soil Biology and Biochemistry*, *118*, 115–129. https://doi.org/10.1016/j.soilbio.2017.12.010

Estop-Aragones, C., Czimczik, C. I., Heffernan, L., Gibson, C., Walker, J. C., Xu, X. M., & Olefeldt, D. (2018). Respiration of aged soil carbon during fall in permafrost peatlands enhanced by active layer deepening following wildfire but limited following thermokarst. *Environmental Research Letters*, *13*(8). https://doi.org/10.1088/1748-9326/aad5f0

Flynn, W. (1968). The determination of low levels of polonium-210 in environmental materials. *Analytica Chimica Acta*, *43*, 221–227. https://doi.org/10.1016/s0003-2670(00)89210-7

Forster, P., Storelvmo, T., Armour, K., Collins, W., Dufresne, J. L., Frame, D., et al. (2021). The Earth's energy budget, climate feedbacks, and climate sensitivity. In V. Masson-Delmotte, P. Zhai, A. Pirani, S. L. Connors, C. Péan, S. Berger, N. Caud, Y. Chen, L. Goldfarb, M. I. Gomis, M. Huang, K. Leitzell, E. Lonnoy, J. B. R. Matthews, T. K. Maycock, T. Waterfield, O. Yelekçi, R. Yu, & B. Zho (Eds.), *Climate change 2021: The physical science basis. Contribution of working group I to the sixth assessment report of the intergovernmental panel on climate change*. Cambridge University Press. In Press.

Freeman, C., Evans, C., Monteith, D., Reynolds, B., & Fenner, N. (2001). Export of organic carbon from peat soils. *Nature*, *412*(6849). 785–785. https://doi.org/10.1038/35090628

Freeman, C., Fenner, N., Ostle, N., Kang, H., Dowrick, D., Reynolds, B., et al. (2004). Export of dissolved organic carbon from peatlands under elevated carbon dioxide levels. *Nature*, *430*(6996), 195–198. https://doi.org/10.1038/nature02707

Frolking, S., Talbot, J., & Subin, Z. M. (2014). Exploring the relationship between peatland net carbon balance and apparent carbon accumulation rate at century to millennial time scales. *The Holocene*, *24*(9), 1167–1173. https://doi.org/10.1177/0959683614538078

Fudyma, J. D., Lyon, J., AminiTabrizi, R., Gieschen, H., Chu, R. K., Hoyt, D. W., et al. (2019). Untargeted metabolomic profiling of *Sphagnum fallax* reveals novel antimicrobial metabolites. *Plant Direct*, *3*(11). https://doi.org/10.1002/pld3.179

Goslar, T., van der Knaap, W. O., Hicks, S., Andriĉ, M., Czernik, J., Goslar, E., et al. (2005). Radiocarbon dating of modern peat profiles: Pre- and post-bomb ^{14}C variations in the construction of age-depth models. *Radiocarbon*, *47*(1), 115–134. https://doi.org/10.1017/s0033822200052243

Grant, R. F., Mekonnen, Z. A., Riley, W. J., Arora, B., & Torn, M. S. (2019). Modeling climate change impacts on an Arctic polygonal tundra: 2. Changes in CO_2 and CH_4 exchange depend on rates of permafrost thaw as affected by changes in vegetation and drainage. *Journal of Geophysical Research: Biogeosciences*, *124*(5), 1323–1341. https://doi.org/10.1029/2018jg004645

Heffernan, L., Estop-Aragones, C., Knorr, K. H., Talbot, J., & Olefeldt, D. (2020). Long-term impacts of permafrost thaw on carbon storage in peatlands: Deep losses offset by surficial accumulation. *Journal of Geophysical Research: Biogeosciences*, *125*(3), e2019JG005501. https://doi.org/10.1029/2019jg005501

Hodgkins, S. B., Tfaily, M. M., McCalley, C. K., Logan, T. A., Crill, P. M., Saleska, S. R., et al. (2014). Changes in peat chemistry associated with permafrost thaw increase greenhouse gas production. *Proceedings of the National Academy of Sciences of the United States of America*, *111*(16), 5819–5824. https://doi.org/10.1073/pnas.1314641111

Hodgkins, S. B., Tfaily, M. M., Podgorski, D. C., McCalley, C. K., Saleska, S. R., Crill, P. M., et al. (2016). Elemental composition and optical properties reveal changes in dissolved organic matter along a permafrost thaw chronosequence in a subarctic peatland. *Geochimica et Cosmochimica Acta*, *187*, 123–140. https://doi.org/10.1016/j.gca.2016.05.015

Hua, Q., Barbetti, M., & Rakowski, A. Z. (2013). Atmospheric radiocarbon for the period 1950–2010. *Radiocarbon*, *55*(4), 2059–2072. https://doi.org/10.2458/azu_js_rc.v55i2.16177

Hugelius, G., Strauss, J., Zubrzycki, S., Harden, J. W., Schuur, E., Ping, C.-L., et al. (2014). Estimated stocks of circumpolar permafrost carbon with quantified uncertainty ranges and identified data gaps. *Biogeosciences*, *11*(23), 6573–6593. https://doi.org/10.5194/bg-11-6573-2014

Jammet, M., Dengel, S., Kettner, E., Parmentier, F., Wik, M., Crill, P. M., & Friborg, T. (2017). Year-round CH_4 and CO_2 flux dynamics in two contrasting freshwater ecosystems of the subarctic. *Biogeosciences*, *14*(22), 5189–5216. https://doi.org/10.5194/bg-14-5189-2017

Johansson, T., Malmer, N., Crill, P. M., Friborg, T., Åkerman, J. H., Mastepanov, M., & Christensen, T. R. (2006). Decadal vegetation changes in a northern peatland, greenhouse gas fluxes and net radiative forcing. *Global Change Biology*, *12*(12), 2352–2369. https://doi.org/10.1111/j.1365-2486.2006.01267.x

Jones, M. C., Booth, R. K., Yu, Z. C., & Ferry, P. (2013). A 2200-year record of permafrost dynamics and carbon cycling in a collapse-scar bog, interior Alaska. *Ecosystems*, *16*(1), 1–19. https://doi.org/10.1007/s10021-012-9592-5

Jones, M. C., Harden, J., O'Donnell, J., Manies, K., Jorgenson, T., Treat, C., & Ewing, S. (2017). Rapid carbon loss and slow recovery following permafrost thaw in boreal peatlands. *Global Change Biology*, *23*(3), 1109–1127. https://doi.org/10.1111/gcb.13403

Kokfelt, U., Reuss, N., Struyf, E., Sonesson, M., Rundgren, M., Skog, G., & Hammarlund, D. (2010). Wetland development, permafrost history and nutrient cycling inferred from late Holocene peat and lake sediment records in subarctic Sweden. *Journal of Paleolimnology*, *44*(1), 327–342. https://doi.org/10.1007/s10933-010-9406-8

Kokfelt, U., Rosén, P., Schoning, K., Christensen, T. R., Förster, J., Karlsson, J., et al. (2009). Ecosystem responses to increased precipitation and permafrost decay in subarctic Sweden inferred from peat and lake sediments. *Global Change Biology*, *15*, 1652–1663. https://doi.org/10.1111/j.1365-2486.2009.01880.x

Lee, H., Schuur, E. A. G., Inglett, K. S., Lavoie, M., & Chanton, J. P. (2012). The rate of permafrost carbon release under aerobic and anaerobic conditions and its potential effects on climate. *Global Change Biology*, *18*(2), 515–527. https://doi.org/10.1111/j.1365-2486.2011.02519.x

MacDonald, G. M., Beilman, D. W., Kremenetski, K. V., Sheng, Y., Smith, L. C., & Velichko, A. A. (2006). Rapid early development of circumarctic peatlands and atmospheric CH_4 and CO_2 variations. *Science*, *314*(5797), 285–288. https://doi.org/10.1126/science.1131722

MacDougall, A. H., Avis, C. A., & Weaver, A. J. (2012). Significant contribution to climate warming from the permafrost carbon feedback. *Nature Geoscience*, *5*(10), 719–721. https://doi.org/10.1038/ngeo1573

Malhotra, A., Moore, T. R., Limpens, J., & Roulet, N. T. (2018). Post-thaw variability in litter decomposition best explained by microtopography at an ice-rich permafrost peatland. *Arctic, Antarctic, and Alpine Research*, *50*(1). https://doi.org/10.1080/15230430.2017.1415622

Malhotra, A., & Roulet, N. (2015). Environmental correlates of peatland carbon fluxes in a thawing landscape: Do transitional thaw stages matter? *Biogeosciences*, *12*(10), 3119–3130. https://doi.org/10.5194/bg-12-3119-2015

Malmer, N., Johansson, T., Olsrud, M., & Christensen, T. (2005). Vegetation, climatic changes and net carbon sequestration in a North-Scandinavian subarctic mire over 30 years. *Global Change Biology*, *11*(11), 1895–1909.

Malmer, N., & Wallén, B. (1996). Peat formation and mass balance in subarctic ombrotrophic peatland around Abisko, northern Scandinavia. *Ecological Bulletins*, 79–92.

Martin, E. A., & Rice, C. A. (1981). *Sampling and analyzing sediment cores for ^{210}Pb geochronology*. (U.S. Geological Survey Open File Report 81-983). https://doi.org/10.3133/ofr81983. report

McCalley, C. K., Woodcroft, B. J., Hodgkins, S. B., Wehr, R. A., Kim, E.-H., Mondav, R., et al. (2014). Methane dynamics regulated by microbial community response to permafrost thaw. *Nature*, *514*(7523), 478–481. https://doi.org/10.1038/nature13798

McGuire, A. D., Lawrence, D. M., Koven, C., Clein, J. S., Burke, E., Chen, G., et al. (2018). Dependence of the evolution of carbon dynamics in the northern permafrost region on the trajectory of climate change. *Proceedings of the National Academy of Sciences of the United States of America*, *115*(15), 3882–3887. https://doi.org/10.1073/pnas.1719903115

Mekonnen, Z. A., Riley, W. J., & Grant, R. F. (2018). 21st century tundra shrubification could enhance net carbon uptake of North America Arctic tundra under an RCP8. 5 climate trajectory. *Environmental Research Letters*, *13*(5), 054029. https://doi.org/10.1088/1748-9326/aabf28

Mishra, U., Drewniak, B., Jastrow, J. D., Matamala, R. M., & Vitharana, U. W. A. (2017). Spatial representation of organic carbon and active-layer thickness of high latitude soils in CMIP5 earth system models. *Geoderma*, *300*, 55–63. https://doi.org/10.1016/j.geoderma.2016.04.017

Natali, S. M., Schuur, E. A., Trucco, C., Hicks Pries, C. E., Crummer, K. G., & Baron Lopez, A. F. (2011). Effects of experimental warming of air, soil and permafrost on carbon balance in Alaskan tundra. *Global Change Biology*, *17*(3), 1394–1407. https://doi.org/10.1111/j.1365-2486.2010.02303.x

O'Donnell, J. A., Jorgenson, M. T., Harden, J. W., McGuire, A. D., Kanevskiy, M. Z., & Wickland, K. P. (2012). The effects of permafrost thaw on soil hydrologic, thermal, and carbon dynamics in an Alaskan peatland. *Ecosystems*, *15*(2), 213–229.

Oldfield, F., Appleby, P., Cambray, R., Eakins, J., Barber, K., Battarbee, R., et al. (1979). ^{210}Pb, ^{137}Cs and ^{239}Pu profiles in ombrotrophic peat. *Oikos*, *33*, 40–45. https://doi.org/10.2307/3544509

Olefeldt, D., & Roulet, N. (2012). Effects of permafrost and hydrology on the composition and transport of dissolved organic carbon in a subarctic peatland complex. *Journal of Geophysical Research*, *117*(G1), G01005. https://doi.org/10.1029/2011jg001819

Olefeldt, D., Roulet, N. T., Bergeron, O., Crill, P. M., Backstrand, K., & Christensen, T. R. (2012). Net carbon accumulation of a high-latitude permafrost palsa mire similar to permafrost-free peatlands. *Geophysical Research Letters*, *39*, L03501. https://doi.org/10.1029/2011gl050355

Olefeldt, D., Turetsky, M. R., Crill, P. M., & McGuire, A. D. (2013). Environmental and physical controls on northern terrestrial methane emissions across permafrost zones. *Global Change Biology*, *19*(2), 589–603. https://doi.org/10.1111/gcb.12071

Olid, C., Klaminder, J., Monteux, S., Johansson, M., & Dorrepaal, E. (2020). Decade of experimental permafrost thaw reduces turnover of young carbon and increases losses of old carbon, without affecting the net carbon balance. *Global Change Biology*, *26*, 5886–5898. https://doi.org/10.1111/gcb.15283

Olid, C., Nilsson, M. B., Eriksson, T., & Klaminder, J. (2014). The effects of temperature and nitrogen and sulfur additions on carbon accumulation in a nutrient-poor boreal mire: Decadal effects assessed using ^{210}Pb peat chronologies. *Journal of Geophysical Research: Biogeosciences*, *119*(3), 392–403. https://doi.org/10.1002/2013jg002365

Pelletier, N., Talbot, J., Olefeldt, D., Turetsky, M., Blodau, C., Sonnentag, O., & Quinton, W. L. (2017). Influence of Holocene permafrost aggradation and thaw on the paleoecology and carbon storage of a peatland complex in northwestern Canada. *The Holocene*, *27*(9), 1391–1405. https://doi.org/10.1177/0959683617693899

Preiss, N., Mélières, M. A., & Pourchet, M. (1996). A compilation of data on lead 210 concentration in surface air and fluxes at the air-surface and water-sediment interfaces. *Journal of Geophysical Research*, *101*(D22), 28847–28862. https://doi.org/10.1029/96jd01836

Ratcliffe, J., Andersen, R., Anderson, R., Newton, A., Campbell, D., Mauquoy, D., & Payne, R. (2018). Contemporary carbon fluxes do not reflect the long-term carbon balance for an Atlantic blanket bog. *The Holocene*, *28*(1), 140–149. https://doi.org/10.1177/0959683617715689

R Core Team. (2021). *R: A language and environment for statistical computing*. R Foundation for Statistical Computing. Retrieved from https://www.R-project.org/

Reimer, P. J., Austin, W. E., Bard, E., Bayliss, A., Blackwell, P. G., Ramsey, C. B., et al. (2020). The IntCal20 Northern Hemisphere radiocarbon age calibration curve (0–55 cal kBP). *Radiocarbon*, *62*(4), 725–757. https://doi.org/10.1017/rdc.2020.41

Riley, W., Mekonnen, Z., Tang, J., Zhu, Q., Bouskill, N., & Grant, R. (2021). Non-growing season plant nutrient uptake controls Arctic tundra vegetation composition under future climate. *Environmental Research Letters*, *16*, 074047.

Roulet, N. T., Lafleur, P. M., Richard, P. J. H., Moore, T. R., Humphreys, E. R., & Bubier, J. (2007). Contemporary carbon balance and late Holocene carbon accumulation in a northern peatland. *Global Change Biology*, *13*(2), 397–411. https://doi.org/10.1111/j.1365-2486.2006.01292.x

Saarinen, T. (1996). Biomass and production of two vascular plants in a boreal mesotrophic fen. *Canadian Journal of Botany*, *74*(6), 934–938. https://doi.org/10.1139/b96-116

Schaefer, K., Lantuit, H., Romanovsky, V. E., Schuur, E. A. G., & Witt, R. (2014). The impact of the permafrost carbon feedback on global climate. *Environmental Research Letters*, *9*(8). https://doi.org/10.1088/1748-9326/9/8/085003

Schuur, E. A. G., Abbott, B. W., Bowden, W. B., Brovkin, V., Camill, P., Canadell, J. G., et al. (2013). Expert assessment of vulnerability of permafrost carbon to climate change. *Climatic Change*, *119*(2), 359–374. https://doi.org/10.1007/s10584-013-0730-7

Seppälä, M. (2003). Surface abrasion of palsas by wind action in Finnish Lapland. *Geomorphology*, *52*, 141–148.

Silvola, J., Alm, J., Ahlholm, U., Nykanen, H., & Martikainen, P. J. (1996). CO_2 fluxes from peat in boreal mires under varying temperature and moisture conditions. *Journal of Ecology*, *84*(2), 219–228. https://doi.org/10.2307/2261357

Sim, T. G., Swindles, G. T., Morris, P. J., Baird, A. J., Cooper, C. L., Gallego-Sala, A. V., et al. (2021). Divergent responses of permafrost peatlands to recent climate change. *Environmental Research Letters*, *16*(3), 034001. https://doi.org/10.1088/1748-9326/abe00b

Stuiver, M., & Polach, H. A. (1977). Discussion reporting of C-14 data. *Radiocarbon*, *19*(3), 355–363. https://doi.org/10.1017/s0033822200003672

Svensson, B. H., Christensen, T. R., Johansson, E., & Oquist, M. (1999). Interdecadal changes in CO_2 and CH_4 fluxes of a subarctic mire: Stordalen revisited after 20 years. *Oikos*, *85*(1), 22–30. https://doi.org/10.2307/3546788

Tarnocai, C., Canadell, J. G., Schuur, E. A. G., Kuhry, P., Mazhitova, G., & Zimov, S. (2009). Soil organic carbon pools in the northern circumpolar permafrost region. *Global Biogeochemical Cycles*, *23*, GB2023. https://doi.org/10.1029/2008gb003327

Treat, C. C., & Frolking, S. (2013). Carbon storage: A permafrost carbon bomb? *Nature Climate Change*, *3*(10), 865–867. https://doi.org/10.1038/nclimate2010

Treat, C. C., Jones, M. C., Camill, P., Gallego-Sala, A., Garneau, M., Harden, J. W., et al. (2016). Effects of permafrost aggradation on peat properties as determined from a pan-Arctic synthesis of plant macrofossils. *Journal of Geophysical Research: Biogeosciences*, *121*(1), 78–94. https://doi.org/10.1002/2015jg003061

Turetsky, M. R., Abbott, B. W., Jones, M. C., Anthony, K. W., Olefeldt, D., Schuur, E. A. G., et al. (2020). Carbon release through abrupt permafrost thaw. *Nature Geoscience*, *13*(2), 138–143. https://doi.org/10.1038/s41561-019-0526-0

Turetsky, M. R., Wieder, R. K., Vitt, D. H., Evans, R. J., & Scott, K. D. (2007). The disappearance of relict permafrost in boreal North America: Effects on peatland carbon storage and fluxes. *Global Change Biology*, *13*(9), 1922–1934. https://doi.org/10.1111/j.1365-2486.2007.01381.x

Urban, N. R., Eisenreich, S. J., Grigal, D. F., & Schurr, K. T. (1990). Mobility and diagenesis of Pb and Pb-210 in peat. *Geochimica et Cosmochimica Acta*, *54*(12), 3329–3346. https://doi.org/10.1016/0016-7037(90)90288-v

Varner, R. K., Crill, P. M., Frolking, S., McCalley, C. K., Burke, S. A., Chanton, J. P.Isogenie Project Coordinators, et al. (2021). Permafrost thaw driven changes in hydrology and vegetation cover increase trace gas emissions and climate forcing in Stordalen Mire from 1970-2014. *Philosophical Transactions of the Royal Society A*, *380*.

Verhoeven, J. T. A., & Liefveld, W. M. (1997). The ecological significance of organochemical compounds in Sphagnum. *Acta Botanica Neerlandica*, *46*(2), 117–130. https://doi.org/10.1111/plb.1997.46.2.117

Vogel, J. S., Southon, J. R., Nelson, D. E., & Brown, T. A. (1984). Performance of catalytically condensed carbon for use in accelerator mass-spectrometry. *Nuclear Instruments and Methods in Physics Research Section B: Beam Interactions with Materials and Atoms*, *5*(2), 289–293. https://doi.org/10.1016/0168-583x(84)90529-9

von Deimling, T. S., Grosse, G., Strauss, J., Schirrmeister, L., Morgenstern, A., Schaphoff, S., et al. (2015). Observation-based modelling of permafrost carbon fluxes with accounting for deep carbon deposits and thermokarst activity. *Biogeosciences*, *12*(11), 3469–3488. https://doi.org/10.5194/bg-12-3469-2015

Whiting, G. J., & Chanton, J. P. (1993). Primary production control of methane emission from wetlands. *Nature*, *364*(6440), 794–795. https://doi.org/10.1038/364794a0

Wilson, R. M., Fitzhugh, L., Whiting, G. J., Frolking, S., Harrison, M. D., Dimova, N., et al. (2017). Greenhouse gas balance over thaw-freeze cycles in discontinuous zone permafrost. *Journal of Geophysical Research: Biogeosciences*, *122*(2), 387–404. https://doi.org/10.1002/2016jg003600

Wilson, R. M., Hopple, A. M., Tfaily, M. M., Sebestyen, S. D., Schadt, C. W., Pfeifer-Meister, L., et al. (2016). Stability of peatland carbon to rising temperatures. *Nature Communications*, *7*(1). https://doi.org/10.1038/ncomms13723

Wilson, R. M., Neumann, R. B., Crossen, K. B., Raab, N. M., Hodgkins, S. B., Saleska, S. R., et al. (2019). Microbial community analyses inform geochemical reaction network models for predicting pathways of greenhouse gas production. *Frontiers in Earth Science*, *7*(59). https://doi.org/10.3389/feart.2019.00059

Wilson, R. M., Tfaily, M. M., Kolton, M., Johnston, E. R., Petro, C., Zalman, C. A., et al. (2021). Soil metabolome response to whole-ecosystem warming at the Spruce and peatland responses under changing environments experiment. *Proceedings of the National Academy of Sciences of the United States of America*, *118*(25). https://doi.org/10.1073/pnas.2004192118

Wilson, R. M., Zayed, A. A., Crossen, K. B., Woodcroft, B., Tfaily, M. M., Emerson, J., et al. (2021). Functional capacities of microbial communities to carry out large scale geochemical processes are maintained during ex situ anaerobic incubation. *PLoS One*, *16*(2). https://doi.org/10.1371/journal.pone.0245857

Young, D. M., Baird, A. J., Charman, D. J., Evans, C. D., Gallego-Sala, A. V., Gill, P. J., et al. (2019). Misinterpreting carbon accumulation rates in records from near-surface peat. *Scientific Reports*, *9*(1), 17939. https://doi.org/10.1038/s41598-019-53879-8

Yu, Z. (2011). Holocene carbon flux histories of the world's peatlands:Global carbon-cycle implications. *The Holocene*, *21*(5), 761–774. https://doi.org/10.1177/0959683610386982

Yu, Z. C. (2012). Northern peatland carbon stocks and dynamics: A review. *Biogeosciences*, *9*(10), 4071–4085. https://doi.org/10.5194/bg-9-4071-2012

Yu, Z. C., Beilman, D. W., & Jones, M. C. (2009). Sensitivity of northern peatland carbon dynamics to Holocene climate change. In A. J. Baird, L. R. Belyea, X. Comas, A. S. Reeve, & L. D. Slater (Eds.), *Carbon cycling in northern peatlands* (Vol. 184, pp. 55–69).

Zimov, S. A., Davydov, S. P., Zimova, G. M., Davydova, A. I., Schuur, E. A. G., Dutta, K., & Chapin, F. S. (2006). Permafrost carbon: Stock and decomposability of a globally significant carbon pool. *Geophysical Research Letters*, *33*(20), L20502. https://doi.org/10.1029/2006gl027484